Tampere University

Yahya Maly

COLD SPRAYED SLIPS COATINGS

A pathway towards process optimization and icephobicity

Faculty of Engineering and
Natural Sciences
Master's Thesis
May 2020

ABSTRACT

Yahya Maly
Cold Sprayed SLIPS Coatings: A pathway towards process optimization and icephobicity
Master's Thesis
Tampere University
Engineering Materials Science
May 2020

Ice accretion is a major problem that causes economic loss, damages structure, impedes transports, and potentially leads to human injury and death. There is a strong demand for a reliable passive anti-icing system to reduce and prevent ice adhesion, especially in aircraft applications where ice accretion can change the aerodynamic behaviour and lead to loss of control. Although de-icing and active anti-icing methods exist, passive anti-icing systems are desired because they do not rely on complicated infrastructure and do not require externally supplied energy.

It has been established that SLIPS, short for Slippery Liquid-Infused Porous Surfaces, inhibit high water resistance properties, however the connection between the wetting properties (hydrophobicity) and icephobic behavior is under debate. During this study, the feasibility of producing SLIPS via cold spray is studied through multiple randomized experiments aimed at evaluating different spraying parameters and techniques for process development. The study is conducted using various polymer powders and different spraying material. The purpose of these experiments is to produce a functional porous coating that it capable of a lubricant liquid infusion. The process used to produce the polymer-based cold sprayed SLIPS was detailed in this paper.

In total, 34 substrates were cold sprayed with polymer-based powders using low-pressure and high-pressure cold spray guns. Eight samples were selected to undergo lubricant infusion and further testing. The coating structures were visually analysed with a microscope. The wettability was estimated by measuring water contact angle. Roughness data and surface topographies were obtained via a profilometer. Lubricant stability of the oil-infused structures was evaluated via centrifuge testing. The results showed that the production of polymer-based cold sprayed SLIPS is feasible. Furthermore, the cold spraying process aids with the production of SLIPS due to partial melting of the polymer particles upon impact with the substrate, resulting in a porous structure. The result further showed that cold sprayed SLIPS have excellent oil stability and do not require complicated surface preparation, which is advantageous over other SLIPS design methods.

This thesis work focused on the development of coatings for potential use as icephobic products (i.e. passive anti-icing systems). A deeper investigation into icephobics found that since 1930's, the development of icephobic products has been hindered by the lack of understanding of ice accretion, unknown meaningful testing methods for new products, debated connection to hydrophobicity, unreliability of icing wind tunnel testing and lack of a standardized method, large scatters of ice adhesion data, discrepancies in literature and different conclusions on the affecting mechanisms, experimental biases, and a general lack of understanding for properties. Although there exist a few icephobic products on the market, their effectiveness is in question by research.

The results showed that non-infused samples show greater water contact angle yet, comparison of the real wetting behaviour relies on interpreting the apparent contact angle of three interfacial tensions. Additionally, since the wetting behaviour does not directly imply icephobicity, the author of this study could not conclude that the produced coatings are icephobic, but nevertheless recommended additional testing of polymer-based cold sprayed SLIPS in future studies.

Keywords: Icephobicity, Aircraft icing, Ice wind tunnel, Anti-icing, De-icing, Passive anti-ice systems, icephobic coatings, sprayed coatings, hydrophobicity, superhydrophobicity, nature-inspired technology, the Lotus Effect, SLIPS, Slippery Liquid Infused Porous Surfaces, Thermal spraying technology, Cold spraying of polymers, Flame spraying, Process development

PREFACE

This master's thesis was started in January 2020 and finished in May 2020 at the department of Materials Science, Tampere University. The thesis project is funded by Academy of Finland and part of TS-SLIPS (Thermally sprayed slippery liquid infused porous surfaces – towards durable anti-icing coatings).

The coating processing was done in the facilities of TSCF (Thermal Spray Center Finland) at Tampere University. I would like to thank our senior technician Jarkko Lehti for helping with thermal spraying.

Another expression of gratitude goes for Jarmo Laakso for helping with profilometer roughness. The measurements would have been difficult to obtain without your help.

I would like to thank Valentina Donadei and Enni Hartikainen for their comments and advice with contact angle measurements and other tests.

This work was supervised by Dr. Heli Koivuluoto and Dr. Essi Sarlin. I would like to thank them both for their advice.

Finally, I would like to thank my friends and family for their love and support.

Tampere, 27 April 2020

Yahya Maly

CONTENTS

LIST OF SYMBOLS AND ABBREVIATIONS

AEP	Annual Energy Production
HP	High Pressure
HPCS	High Pressure Cold Spray
LP	Low Pressure
LPCS	Low Pressure Cold Spray
RPM	Revolutions per minute
SLIPS	Slippery Liquid-Infused Porous Surfaces
WCA	Water Contact Angle

1. INTRODUCTION

1.1 Effects of ice accretion

Ice accretion is an undesirable weather condition that affects logistics, industry, infrastructure, outdoor facilities and structures such as airplanes, ships, power plants, telecommunication equipment and residential areas leading to enormous financial loss and structural damage. A few examples of the potentially damaging effect of icing is shown in Figure 1. Icing can cause a massive impact on transportation and reduce efficiency of mechanical systems. Icing in cold climate regions, for example, can cause a loss of Annual Energy Production (AEP) as high as 23% on wind turbine operation [1].

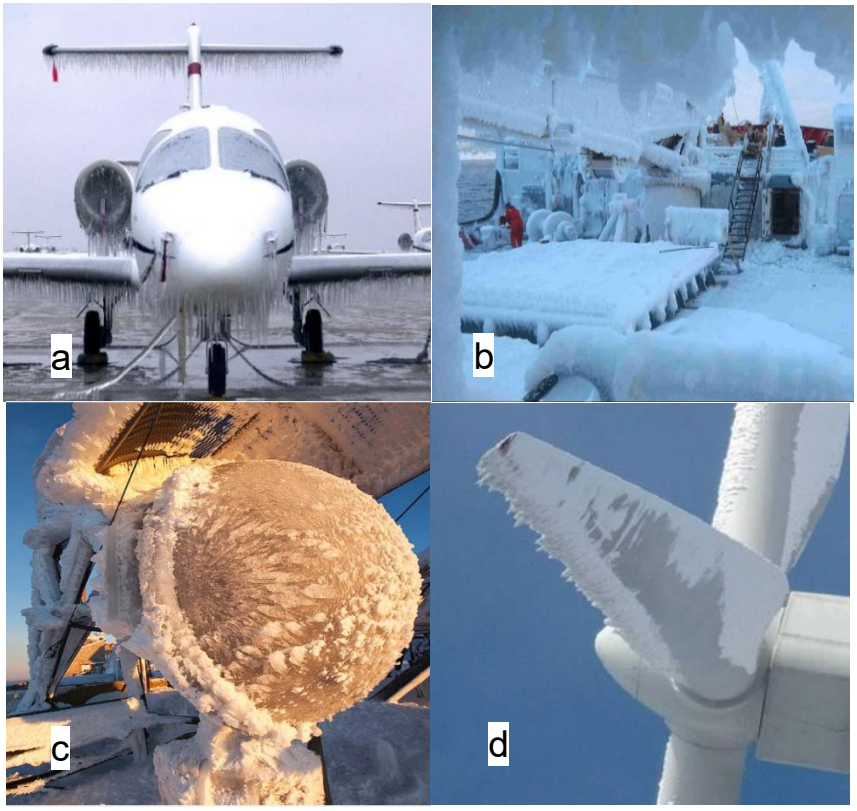

Figure 1. *Ice and snow accumulation can turn efficient mechanical and electronic systems into dysfunctional, rock-like objects. Ice accretion on a) an airplane* [2]*, b) a vessel* [3]*, c) communication equipment* [4]*, and d) wind turbine blade* [5].

Ice accretion can also be a hazardous condition. For example, ice accretion on aircraft frames and unprotected surfaces, as shown in Figure 2a and 2c, affects aerodynamic performance which can ultimately lead to loss of control of the aircraft [6]. Ice also can restrict engine air inlet [6], as shown in Figure 2b, which can lead to engine failures.

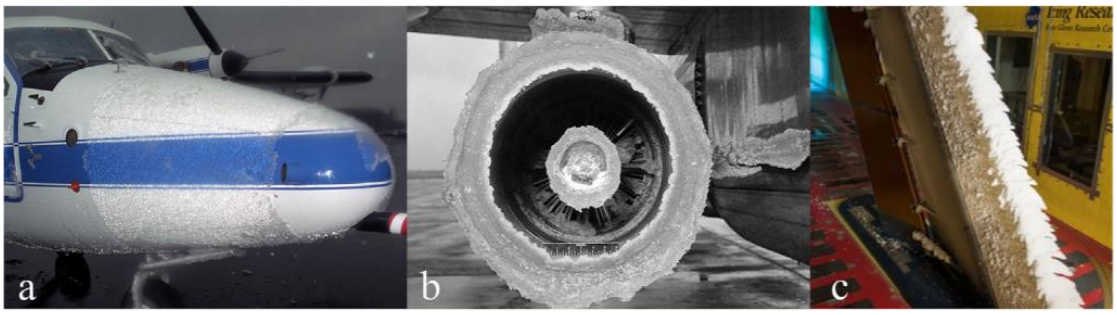

Figure 2. *Ice accretion on (a) aircraft body, (b) aircraft engine and (c) aircraft surfaces. Images are provided by NASA* [7].

Ice can also form, for example, on train breaks as shown in Figure 3a which can jeopardize breaking efficiency [8] and ultimately lead to loss of control and accidents. Ice accretion on train tracks, as shown in Figure 3b, causes wheel slip, interrupts electrical supply on top on the conductor rail, and causes trip delays and cancellations [9].

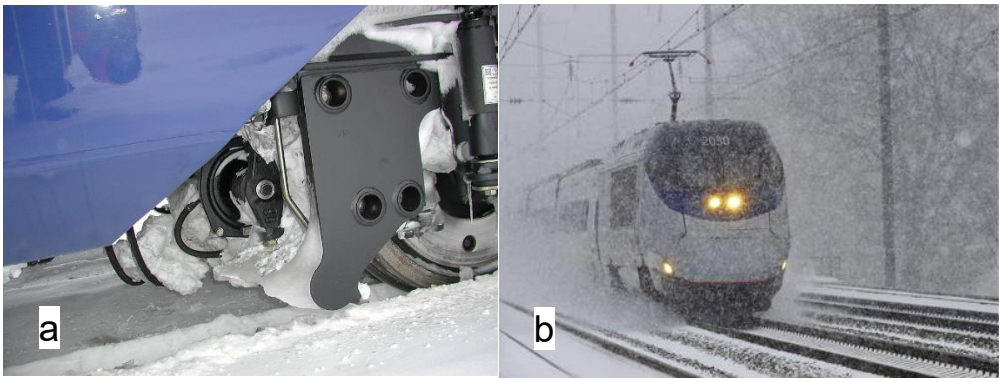

Figure 3. *Ice formation on a) train breaks* [8] *and b) train tracks* [10].

1.2 Anti-icing and de-icing methods

There exist two main methods for dealing with icing problems: anti-icing and de-icing methods. Each method has its own advantages and disadvantages. The several methods can also be used together to prevent and remove snow and ice.

1.2.1 De-icing systems

De-icing is the removal of snow and ice off surfaces by mechanical, thermal or chemical means [8]. An example of de-icing methods includes the physical removal of snow and

ice from aircraft body, as shown in Figure 4. Although de-icing methods are simple, reliable and more common than other methods, they involve complicated infrastructure and require substantial energy [11]. In addition, they cannot be sufficiently used to prevent hazardous conditions. Because of this, there is a demand for anti-icing systems.

Figure 4. *Photographs of current and historical de-icing methods for the removal of ice off aircraft wings* [12].

1.2.2 Anti-icing systems

Anti-icing is preventing ice formation over protected areas; they are more efficient than de-icing methods because in theory they act to prevent snow from bonding rather than break down ice layers [13]. There exist two main types: passive and active. Many are still in development however, there are only a few on the market [14]. Active anti-icing systems require supplied energy like de-icing systems and are mostly used in the aerospace industry [14]. Passive anti-icing methods do not require supplied energy. Examples of researched passive systems include paints and coatings, as shown in Figure 5.

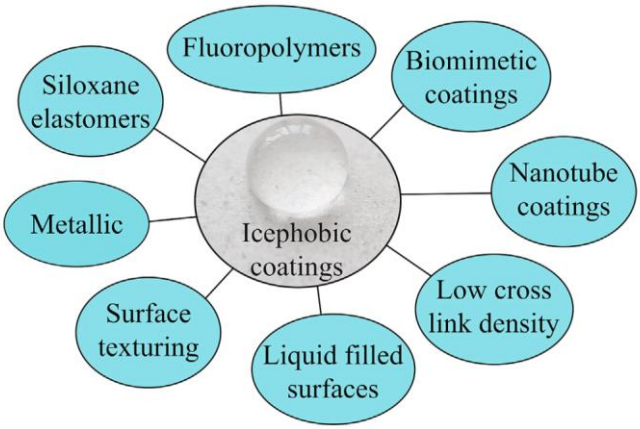

Figure 5. *A schematic of passive anti-icing coatings* [7]. *Note this study focuses on liquid filled surfaces type icephobic coatings.*

1.3 Aim of study

The aim of this study is to evaluate the feasibility of producing cold sprayed, porous, liquid-infusible structures and discuss their potential to be used as icephobic (i.e. passive anti-icing) coatings. Process development parameters are determined based on comparison of randomized test experiments. In addition, water contact angle of the produced coatings is measured. The process of producing cold sprayed SLIPS is described in Figure 6; it involves cold spray-coating a surface or a substrate and infusing it with lubricating liquid. The SLIPS structure can be re-infused as need to maintain function.

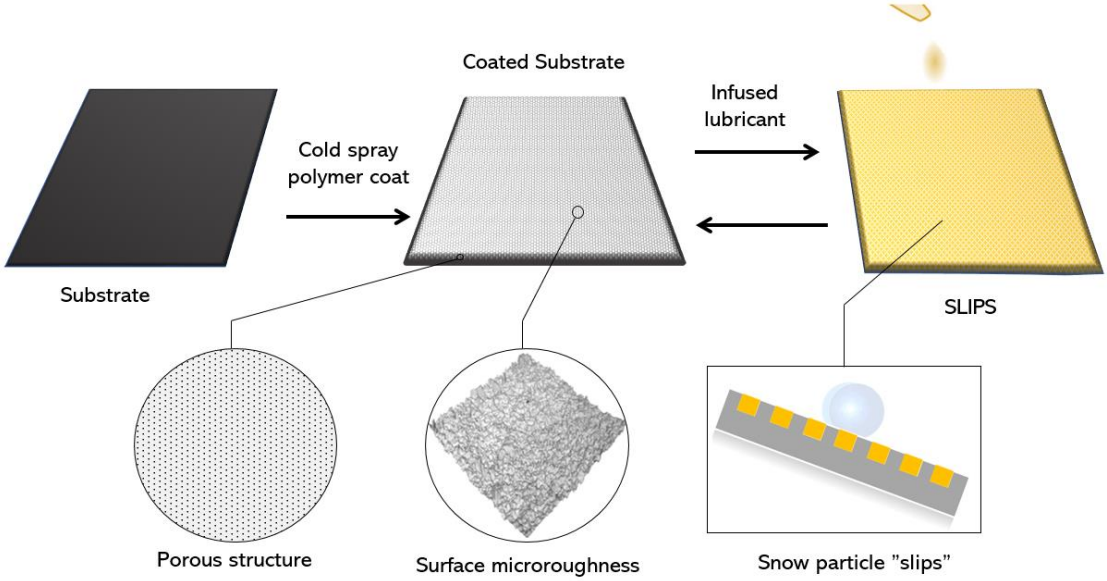

Figure 6. *Cold sprayed SLIPS process: (1) cold spray coating a substrate, (2) infusing the coated surface with oil, and (3) re-infusing as needed.*

2. ICEPHOBICITY AND ICEPHOBIC COATINGS

Icephobicity is a term that is derived from the words ice and phobia (Greek fəʊbɪə, phóbos, meaning “fear” or “aversion to something” [15]). Although the term “icephobicity” is almost exclusively used in research, “aversion to ice,” and “ice-resistance” are commonly supposed meanings. Although there are different descriptions for icephobicity, generally icephobic surface should reduce snow accumulation and prevent ice adhesion on solid surfaces [11]. When discussing icephobicity, the terms “hydrophobicity” and “superhydrophobicity” often come into discussion. To understand the connection, one must become familiar with current research standing on the different phenomena.

2.1 Hydrophobic, superhydrophobic and icephobic surfaces

Hydrophobicity (resistance to water) and superhydrophobicity (high resistance to water) are studied by measuring the contact angle of water droplets or “*Water Contact Angle*” (WCA) [16] for surfaces. Figure 7 explains the process behind WCA measurement of a droplet on a surface. The idea is simple: surfaces which have a measured WCA of 90 degrees or more are said to be hydrophobic, while surface having a WCA of 150 degrees are said to be superhydrophobic [17] (explained in Figure 8). This is a reliable testing method for evaluating hydrophobic and superhydrophobic behavior of surfaces [18].

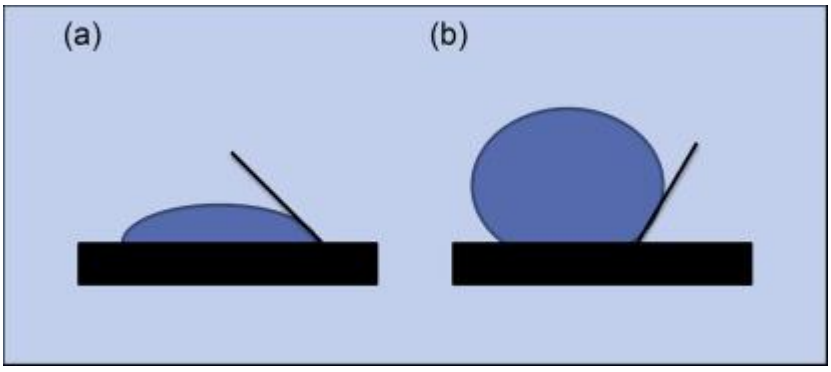

Figure 7. *Contact angle of a water droplet; <90 degrees indicates wetting (a) and ≥90 degrees indicates nonwetting (b)* [19].

Icephobicity, on the other hand, is a poorly understood phenomenon due to the complexity of ice formation on surfaces [20] and unknown reliable and meaningful testing methods [11]. Ice accretion on an aircraft or a moving ship, for example, is much different than ice accretion on a train break or a stationary object. Some research studies select icephobic surfaces based on highly hydrophobic properties [11],[21],[22]. Studies more

commonly link icephobicity with superhydrophobicity based on behavioral similarities between the surfaces [23],[22]. Nevertheless, many opposing research studies conclude that there is no direct relationship between the different phenomena [23].

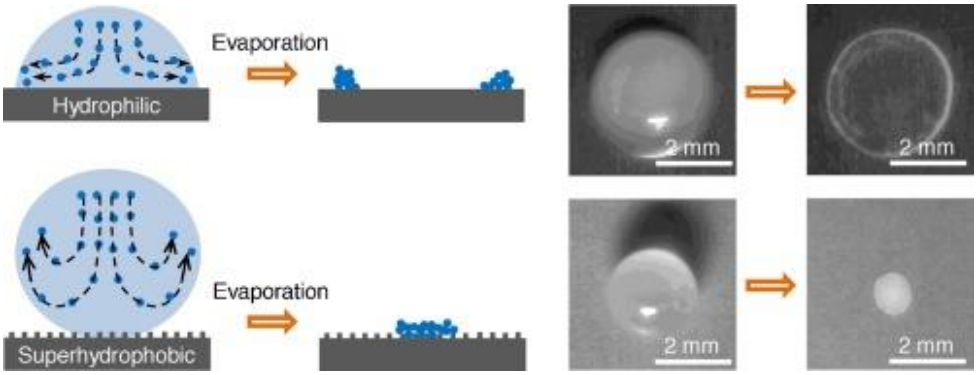

Figure 8. *Superhydrophobic surfaces rely on increased surface roughness of a hydrophobic surface (to create highly hydrophobic air pockets)* [24].

2.2 Testing methods for icephobic surfaces

An existing method for testing icephobic behavior of surfaces involves measuring ice adhesion strength of ice formed in an icing wind tunnel, such as one show in Figure 9, for different surfaces. In theory, it is possible to design experiments based on the most representative atmospheric parameters. Nevertheless, there are technical limitations and a lack of a standardized testing method available for ice wind tunnel testing. Different studies use different ice adhesion methods, ice thicknesses, test conditions and variables [7] which makes comparing different test results impossible. Data obtained from one test are useful in conducting comparative analysis only under exact conditions.

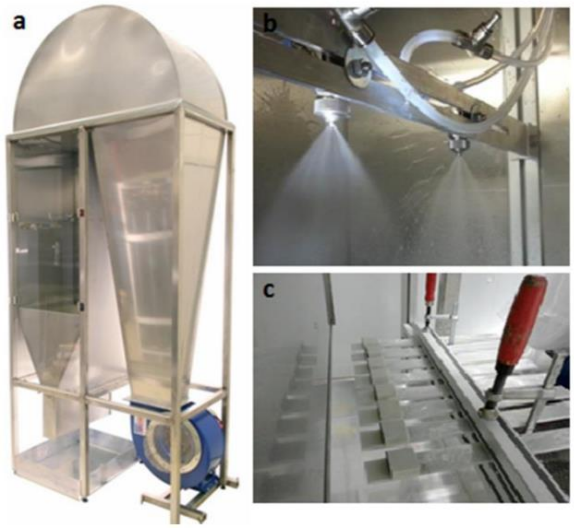

Figure 9. *Icing wind tunnel currently under development at Tampere University (formerly Tampere University of Technology)* [25].

The use of different testing methods in icephobics studies oftentimes leads to large variation of data and ice adhesion test results. Specifically, literature does not agree on a small range of values for ice adhesion strengths for the same individual substrates and surfaces. Literature has reported that, for example, uncoated aluminum has ice adhesion strength values between 55 and 1360 kPa in different studies [26],[27]. Similarly, there exists large scatters in ice adhesion strength data for individual solid surfaces in different studies [28],[29]. This leads to a lack of understanding of icephobic surface properties.

2.3 Properties of icephobic surfaces

Due to the large variation in data, the connection between surface properties and ice adhesion strength is not well established [30]. As icing test data present large scatters [27], there exist discrepancies between studies on the effect of surface properties on ice adhesion strength. For example, the effect of roughness, a key property in surface engineering, on icephobicity is unknown because the interaction of ice with surface roughness is not understood [27]. Most roughness models show large scatters when plotted against ice adhesion, as shown in Figure 10, and do not provide an understanding of the affecting mechanism of ice adhesion [27]. Based on different studies on the effect of properties, it has been reported that roughness improves icephobic behavior [22], reduces icephobic behavior [31], has a major effect on icephobic behavior [32], and has a secondary effect on icephobic behavior [33]. The data obtained from these studies can be biased, for example, by geometric differences in ice formation [27]. Nevertheless, understanding the effect of surface properties is key to designing icephobic surfaces.

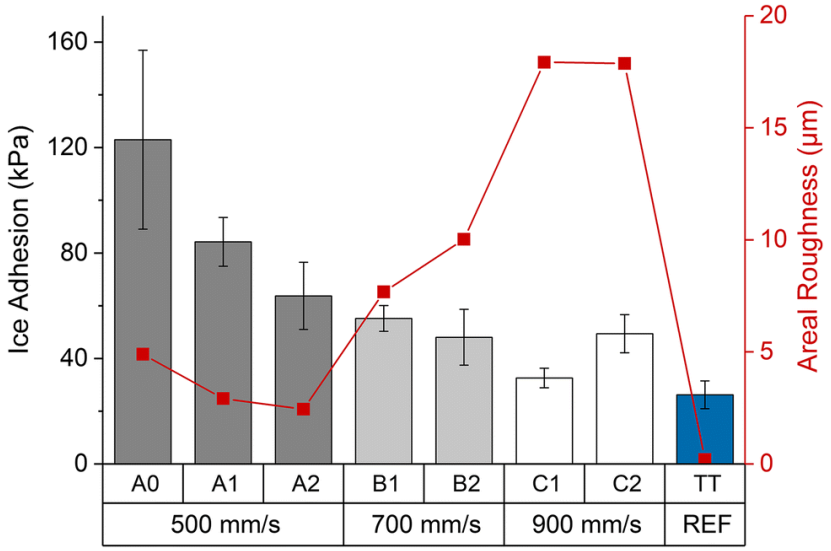

Figure 10. *The adhesion of different material and measured roughness (red dotted line). Graph obtained from Icephobic Behaviour and Thermal Stability of Flame-Sprayed Polyethylene Coating: The Effect of Process Parameters* [34].

Another study conducted on the relationships between ice adhesion and surface roughness found a general relationship between surface roughness and the ice adhesion strength as shown in Figure 11. It was reported that ice adhesion strength increases with increasing roughness, however there was no clear mathematical relationship between roughness and ice adhesion strength [35]. The conclusion of this study is supported by other studies that found similar general increasing relationship [36],[37].

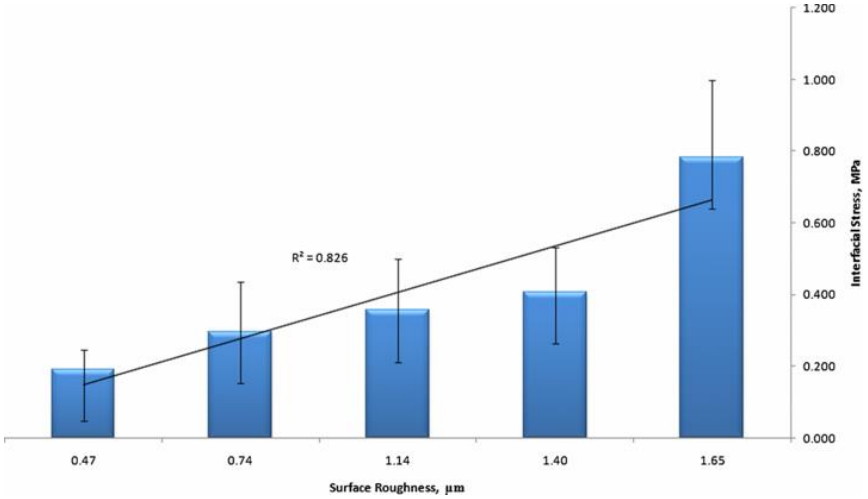

Figure 11. *Surface roughness and ice adhesion strength. Graph obtained from The variation of ice adhesion strength with substrate surface roughness* [35].

A different study published by the American chemical society found that for uncoated glass, the ice adhesion strength decreases with increasing roughness [38] as shown in Figure 12, but an opposite behavior of glass samples coated with silica particles. The study concluded that "the trapped air between water and the superhydrophobic substrates can effectively reduce the ice adhesion and contribute to good durability of the icephobic coating" [38]. These conclusions are closer to studies that support the correlation between icephobicity and high WCA (i.e. the superhydrophobic model) [22].

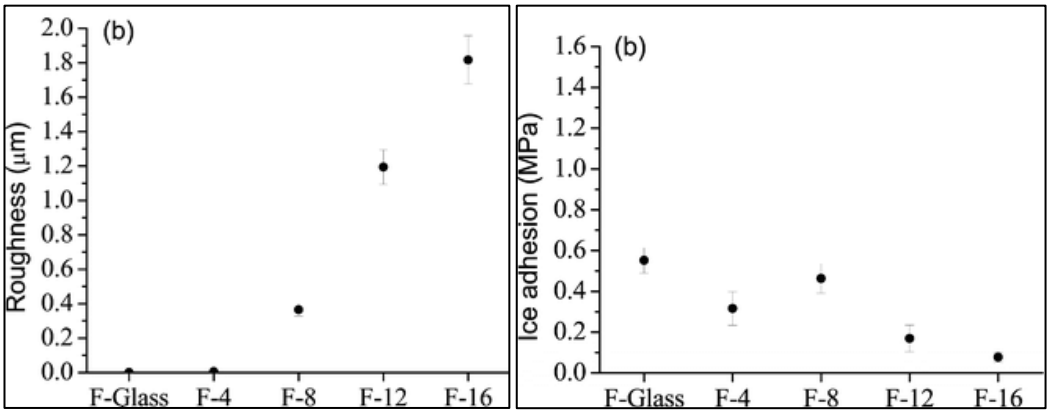

Figure 12*.* *Roughness and ice adhesion of uncoated glass samples* [38]. *Graph obtained from the Development of Sol–Gel Icephobic Coatings.*

2.4 Survey of icephobics research

Besides the lack of understanding ice formation and affecting mechanisms [27], there exists experimental biases and errors which are contributing to misleading conclusions [27]. Based on a survey study, issues facing icephobics studies include the use of different ice adhesion test methods and conditions in different studies, the focus on different study aspects and parameters, and poorly documenting research findings [28]. The survey study highlights that some important parameters are exclusively neglected, ice adhesion data are commonly biased to values different than true values, and there exist other systematic errors leading to different conclusions [28] which should be resolved.

Although these issues are challenging, such errors and biases are harmful and limit the development of evidence-based icephobic solutions for industrial use [29],[27],[39]. While testing and confirming ice adhesion strengths is key to producing icephobic products [27], the comparability element is largely missing which results in a reduced reliability of one set of testing data. As a result of this, it is common that surfaces with low ice adhesion strength (i.e. icephobic) as tested in one icing wind tunnel could be considered non-icephobic (high ice adhesion strength) when tested in another ice wind tunnel.

2.5 Industrial use of icephobic surfaces

The development of an icephobic product is difficult without understanding ice formation and without an acceptable testing method to evaluate these products. Currently, there exists no successful icephobic products available for industry use [40]. According to the author of Progress in Aerospace Sciences, “Combined with the fact that the earliest adhesion tests on low-ice-adhesion surfaces date back to at least the 1930s with no successful commercial product developed to date, there is skepticism in the industry over the effectiveness of new products and no widely accepted method to test them” [25].

Many low friction materials, coatings and paint claimed to eliminate or reduce ice accretion are broadly labeled “icephobic,” yet studies consistently show that these products do not prevent ice buildup any more than any other regular materials do [40]. Because of this, there exists skepticism over their effectiveness [41]. Currently available commercial passive anti-icing systems marked “icephobic” include: Aeropeltechnology AeroPel’s Icephobic [42], Nanosonic HybridShield Icephobic [43], Ecological Coatings 3000 Series Icephobic Coatings [44], and Synavax Icephobic Coatings [45]. Although these products are tested in certain conditions, their effectiveness as “icephobic” products is highly questionable because they are designed based on their highly water resistance properties.

3. NATURE-INSPIRED TECHNOLOGY

As aircrafts face hazardous icing issues (refer to Chapter 1), some of the most exciting and ground-breaking technological solutions are inspired by nature, including the development of aircrafts themselves. In 1903, two American inventors, Wilbur and Orville Wright, achieved the first flight with a powered, sustained and controlled airplane [46] shown in Figure 13, surpassing years of problems confronting aeronautical engineers, pioneers and enthusiasts around the world. The two brothers received patent in America and Europe for their work, despite criticism from the press and aviation community [47].

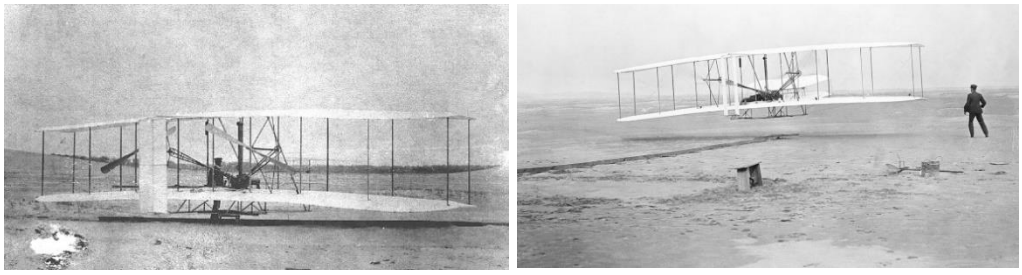

Figure 13. *The first flight of December 17, 1903 near Kitty Hawk, NC* [48].

Although the Wright brothers made a breakthrough in aviation, their vision on how a machine could fly was not at all new. Since ancient times, people observed how birds fly and studied problems of previous flyers (examples of nature-inspired previous fliers are shown in Figure 14). Likewise, the Wright brothers traveled to picnic areas on their bikes to observe how many birds fly around [49]. They modified early kite and glider experiments that did not meet their performance goals, and they built their own models-testing techniques to make a breakthrough flight that changed the future.

Figure 14. *Nature-inspired flying designs: (left) Leonardo da Vinci's 1488 sketch, (right) Jean-Marie Le Bris 1868 flying machine* [50].

Decades later, the same process that the Wright brothers used to build the first successful airplane is still being used by modern-day tech giants like NASA and Airbus to tackle some of the most challenging problems. Today, NASA engineers are making improvements on the original works of Wright Brothers by using computer simulators of their test models [51] to make nature-inspired space exploration. Airbus, a multinational aerospace corporation and the world's largest airline manufacturer, uses nature and concepts of biomimicry to improve performance of modern-day commercial aircrafts [52],[53],[54]. Figure 15 shows future aircraft designs resembling birds, sharks and eagles.

Figure 15. *Airbus studies birds, eagles and sharks to design drag-reducing surfaces, improves aircraft efficiency and reduce emission* [52],[54],[55].

Later problems with aviation and air travel were being resolved with cutting edge, nature-inspired thinking. For example, bionic bones resembling bird bones are being integrated in future airplane design, replacing standard machine structure and windows [56]. Figure 16 compares a bird's bone structure to Airbuse's 2050 airplane design. In a presentation for future projects, Airbus chief engineer explained that bird bones are light and strong and have porous interior structure that carries tension where necessary and leaves space elsewhere [56]. Today's successful aviation leaders have the same vision.

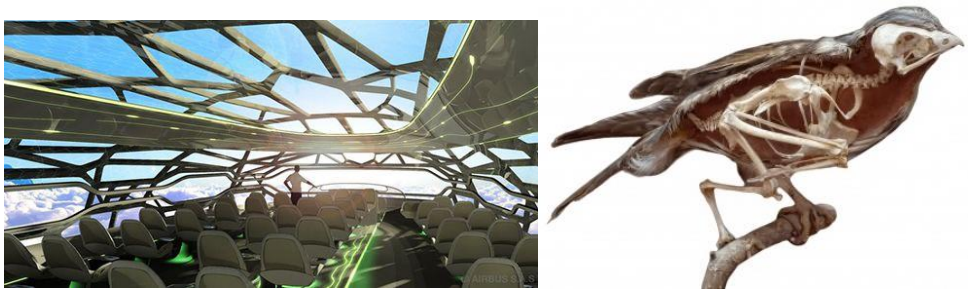

Figure 16. *Airbus's 2050 aircraft structure ("bionic bone design) in comparison to a bird's porous bone structure* [56],[57].

In fact, natural systems are studied to solve many challenging modern-day problems, from producing rechargeable batteries and supercapacitors [58] to developing computer

software [59]. The complexity of a problem requires flexible and adaptable solutions; biological systems, animals and plans have been evolving for millions of years to adapt to many of the same challenges nature poses to us. As such, nature inspired systems are promising to tackle problems with producing icephobic surfaces and structures.

3.1 Slippery Liquid Infused Porous Surface – SLIPS

SLIPS are nature-inspired surfaces designed to repel particles due to their highly slippery, non-stick properties. They show water repellency, self-cleaning and anti-fouling properties [60], like many surfaces found in nature such as the lotus leaf, shark skin and the butterfly wings, shown in Figure 17. The SLIPS design consists of a fabricate surface composed of a structured solid, which function is to hold a liquid layer in place [61]. Ideally, particles that touch these surfaces only meet the lubricating layer (i.e. the oils). And because oils are highly slippery, have no defects and can self-heal, in theory particles can effortlessly and naturally "slip," slide, or roll off these surfaces.

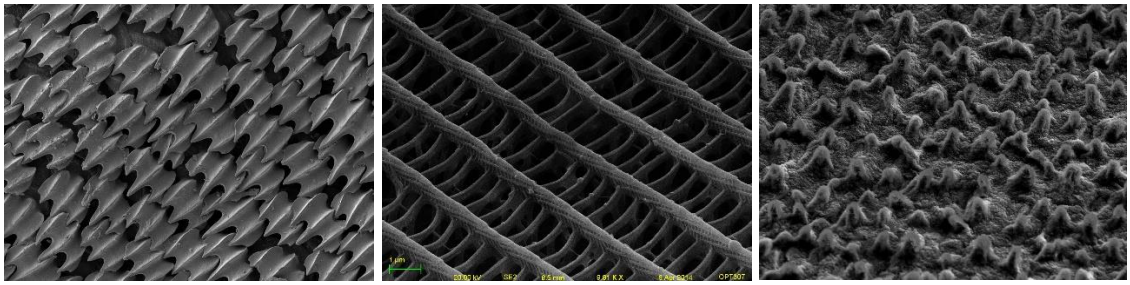

Figure 17. *Microscopic images of shark skin (left), butterfly wings (middle) and the lotus leaf (right)* [62],[63],[64].

3.1.1 The Lotus Effect

The lotus leaf is considered the most notable icon for perfect superhydrophobicity and stable self-cleaning properties; It has led to the invention of a new concept: The Lotus Effect [65]. The lotus leaf has a micro/nanoscale double structure composed of many microscale waxy mastoid processes covered with nanoscale particles (the so-called "hierarchical structure") [60]. This structure design acts to entrap air. And since air is highly hydrophobic, water will naturally roll off the surface, carrying any particles along. The nanoscale particles attach to foreign particles which helps them roll-off effortlessly.

3.1.2 Practical implications

In comparison between the lotus leaf (Figure 18) and other structures, the lotus leaf's papillae (surface asperities) and waxy structure makes for an optimized performance: a perfection of durability and water repellency [65]. Liquid-infused structure rely on com-

plicated process preparation and design for liquid lockability, both considered to be limitations for designing SLIPS [60]. Although the production of a durable and porous structure can be challenging, the structure should be oil-infusible and have good oil-lockability. More recent efforts are incorporating waxes instead of liquids to design structures closer on the lotus effect [66]. Yet, liquid-infused structures are desired in research.

Figure 18. *(left) Water droplets on a lotus leaf* [67] *and (right) a computer graphic showing surface topography of a lotus leaf* [68].

3.1.3 Current SLIPS technology

Current technology dealing with SLIPS aim to overcome challenges with oil lockability and complicated structure preparations. Some examples of recent SLIPS designs are shown in Figure 19. In one example, surface pores are created via laser ablation to avoid sacrificial templates and multi-step preparation processes [69]. The polymer-made, laser ablated SLIPS design by Xi'an Jiaotong University of China is claimed to successfully repel water, hexadecane, milk, Coca-Cola, ink, coffee, fruit juice, glycerol, and egg white [69]. In another example, ferrofluids (i.e. magnetic fluid) are used with magnetic fields to lock the lubricant in place to improve liquid lockability [70].

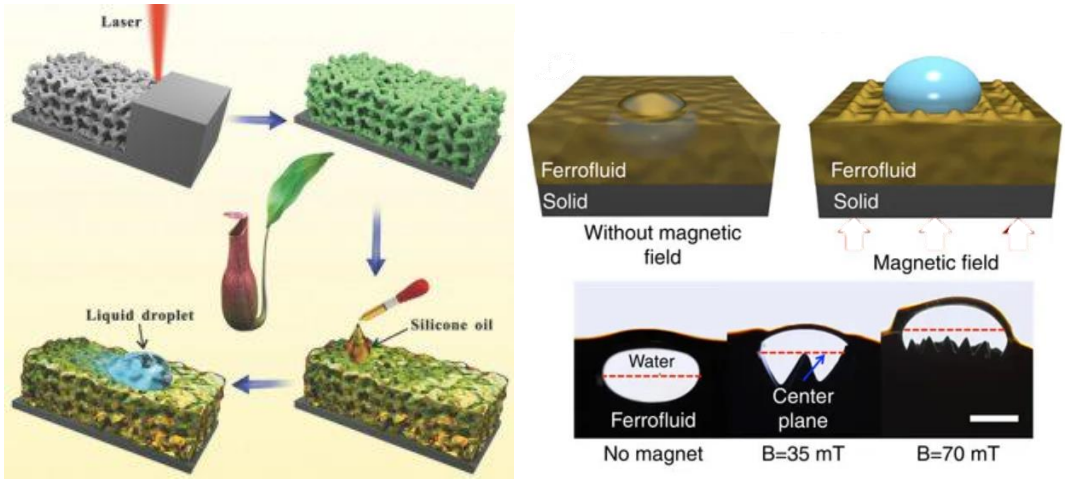

Figure 19. *Example of current SLIPS: (left) Laser ablation of coated structures* [69]*; and (right) Magnetic SLIPS design* [70].

4. THERMALLY SPRAYED POLYMERS

Thermal spraying is a process where material feedstock (powder or bars) are splattered onto a surface adhere by means of thermal energy, mechanical energy or a combination of both. The thermal spraying process started in metal powder production [71]. Yet, thermal spraying of polymers is gaining popularity in various fields including the automotive, aircraft and petrochemical industries [72]. Nevertheless, more existing thermal spraying technologies (i.e. thermal spray guns) are mostly designed for metallic material feedstock. Thermal spray guns for polymers and nozzle are under development.

4.1 Flame/thermal spraying of polymers

Flame spraying is the most typical thermal spraying technique, which relies on transfer of thermal energy (and/or kinetic) to material stock through gas combustion process (Figure 20). The material stock is melted and deposited onto a surface forming a coating [73]. Some specific thermal spraying techniques are based on flame spraying, such as the high-velocity air-fuel spraying (HVAF). Plasma spraying is another variant where material feedstock is melted and deposited through plasma heat transfer. Other types include detonation gun, wire arc spraying, and high-velocity oxygen fuel (HVOF) [74].

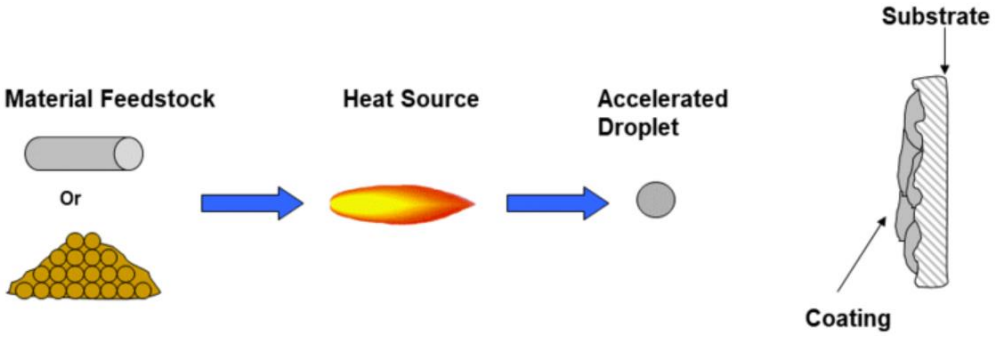

Figure 20. *Thermal spraying process* [74].

4.2 Cold spraying of polymers

Cold spraying is one of the newest thermal spraying techniques; it has gained interest (see trend in Figure 21) especially in surface technology and additive manufacturing [75]. During cold spraying, high velocity, micron-size (typically 10–50 μm in diameter) powder particles deposited in their solid state adhere to a surface via plastic deformation, hence the term “cold spraying” [75]. Unlike other thermal spraying techniques, powder melting

does not occur prior to particle deposition and adhesion mostly relies on kinetic energy. As the particles reach the so called “critical velocity” which depends on the spraying material and substrate properties, they bind to a surface and create a coating [76].

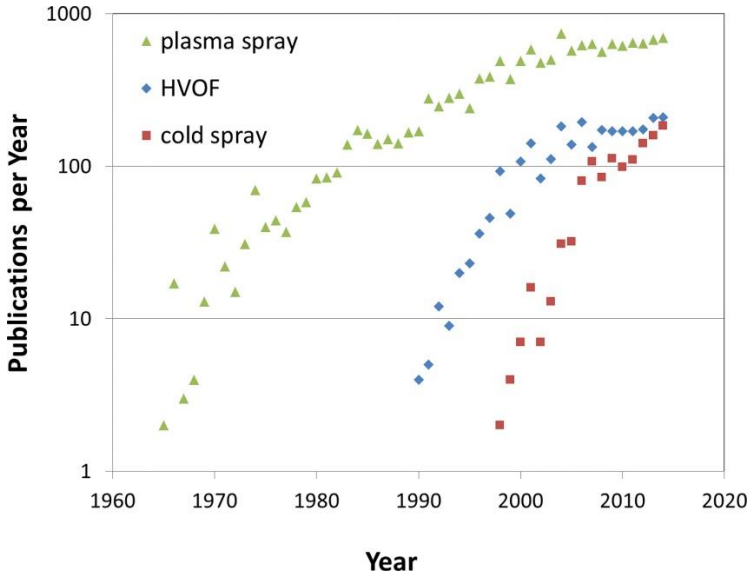

Figure 21. *Cold spraying trend of interest by yearly publications* [75].

Research studies has shown successful cold spraying of metal and metal-ceramic material [75],[77],[78],[79],[80]. Although cold spraying of polymers is not common [75], several studies were conducted cold sprayed polymer materials [81],[82],[83],[84]. Some challenges were reported with powder dispersion and adhesion. As a result, fragile structures, low deposition efficiency, and thin coatings were common issues. Additionally, many cold spraying guns are designed for metallic material applications, even though polymer coatings are becoming increasingly popular in many different fields. As shown in Figure 22, cold spraying requires less energy than other thermal spray types.

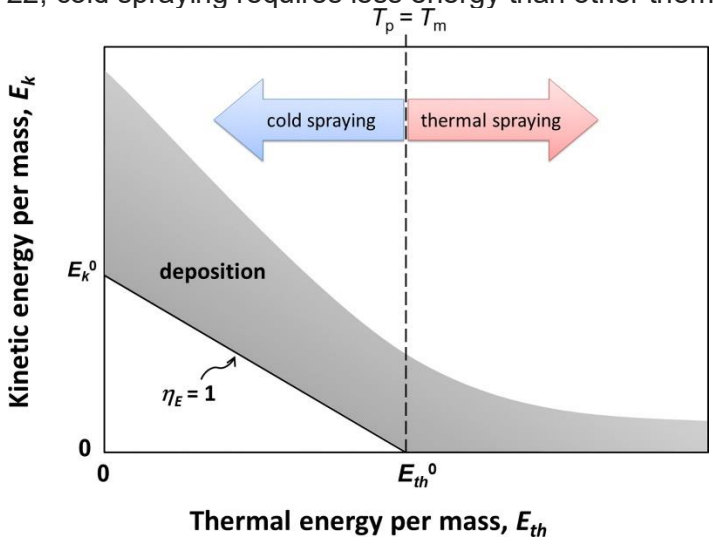

Figure 22. *Energy-based graph of cold spraying. Cold spraying polymers requires less energy than metals/metal-ceramic material* [75].

5. RESEARCH METHODS AND MATERIALS

Appendix A contains information pertaining to process development.

5.1 Spraying material

Polypropylene, PP (Coathylene PB 0580, d50<50 microns, white), thermoplastic polyolefin-based alloy (PPA, PLASCOAT PPA 571 HES, d95<150 grey), Low-density polyethylene (Plascoat LDPE, d95<300 black) and High-density polyethylene (CERAFLOUR 916 HDPE, d50<46, white) powders are sprayed on metallic plate (Low-carbon steel, Fe52, Gritblasted with aluminium oxide F24) using two cold spray guns: high pressure and low pressure. The low-pressure cold spraying (LPCS) gun is DYMET model 403K (Russia) is a high pressure sold spray (HPCS) gun is the Plasma PCS-100 (Japan). The spraying parameters include gas pressure (4,2 to 15 bar), gas temperature (150 to 224°C), powder feeding (3,5 to 4 RPM), substrate temperature (120 to 135°C), spraying speed (manual or 5 to 10 m/min), spray angle (30 to 90°) and number of passes (1 to 3 passes) as tabulated in Table 2 of Results. Pre-trials were conducted using both pressure spray guns. A schematic diagram of cold spraying is shown in Figure 23. Lubricant oil (Dupont Krytox GPL105) is infused in the coating structure via a syringe.

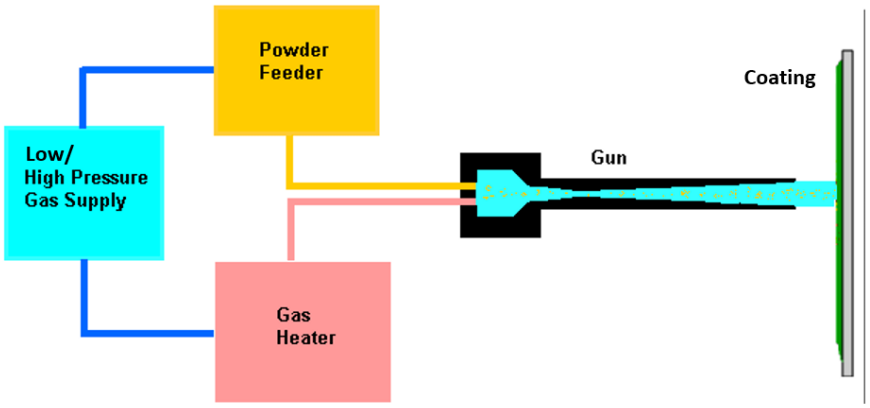

Figure 23. *Schematic diagram of cold spray process. Adapted from Gordon England's Cold Spray Coating process* [85]*. Note that some systems utilize radial powder feeding as opposed to what is shown here (i.e. axial feeding).*

5.2 Pre-heating and plate heating

To facilitate coating adhesion, the substrate is pre-heated to a temperature between 120 and 135°C. Heating the plate continually while spraying is also studied (refer to Appendix A). With plate pre-heating, the substrate is pre heated to a specific temperature using a

gas burner flame gun and, during spraying, is left to cool down. The process is shown in Figure 24. With continuous plate heating, a heating element is installed to the back side of the substrate and the temperature is set to a constant value during spraying. For the selected samples in the Results and Analysis, the substrates were pre heated.

Figure 24 *Pre-heating and spraying (low pressure).*

5.3 Sample preparation

After spraying substrates, a 1x2 cm specimen is cut from samples using Struers Discotom cutter and a 250 mm (10") dia. X 1.5 mm x 32 mm dia Cut-Off Wheel (United States). The specimen is cold mounted using Epofix Kit-box (includes resin, hardener, syringes, cups, stirring sticks). Prior to cold mounting, the specimens are cleaned with ethanol using ultrasonic cleaner. After mounting, the specimen is grinded and polished using Buehler Phoenix 4000 (United States) and Struers Tegramin-30 (United States) sample preparation machines. Fragile coatings prevented preparing all the samples. The mounted samples were then grinded using Buehler Phoenix 4000 (United States) semi-automatic sample preparation machine by holding the samples onto a rotating centrifuge. Finally, the samples were polished using Struers Tegramin-30 (United States) by attaching the samples to the sample holders and selecting the automatic preparation option.

5.4 Testing methods

Various tasting methods are used to study the porous, cold sprayed polymer coating properties and visually examine the structure. Testing methods include studying the structure by microscope, evaluating oil-stability by centrifuge, roughness by profilometer and hydrophobicity by water contact angle. Studying the polymer coat structure is a first

step in evaluating the surface behavior of the polymer coating and achieve the desired function. The purpose of these tests is to basically study the new cold sprayed SLIPS.

5.4.1 Structure by microscope

After sample preparation, specimens are placed under an optical microscope (LEICA DM 2500 M, Germany) to study the structure. The thickness and the porosity are measured using software measurement tools. The coat thickness is calculated based on measured thicknesses at five different regions of the coating. The pore size is calculated based on an average of ten randomly measured pores with standard deviation.

5.4.2 Wetting behaviour by WCA

After stability testing and refilling the samples, the oil-infused samples undergo WCA measurements using the Drop Shape Analyzer – DSA100 (Germany). The samples are placed onto the device and 6 Sessile water droplets with diameters of about 3 to 5 µm are released onto the surface with a needle of 0.5 mm diameter, as shown in Figure 25. The drops are illuminated from one side and a high-quality picture is taken by a camera at the opposite side. The images are transferred to a computer screen and are then analyzed using KRÜSS ADVANCE 1.10.0.34701 software application. Water contact angle measurements are conducted in accordance with the manufacture guidelines.

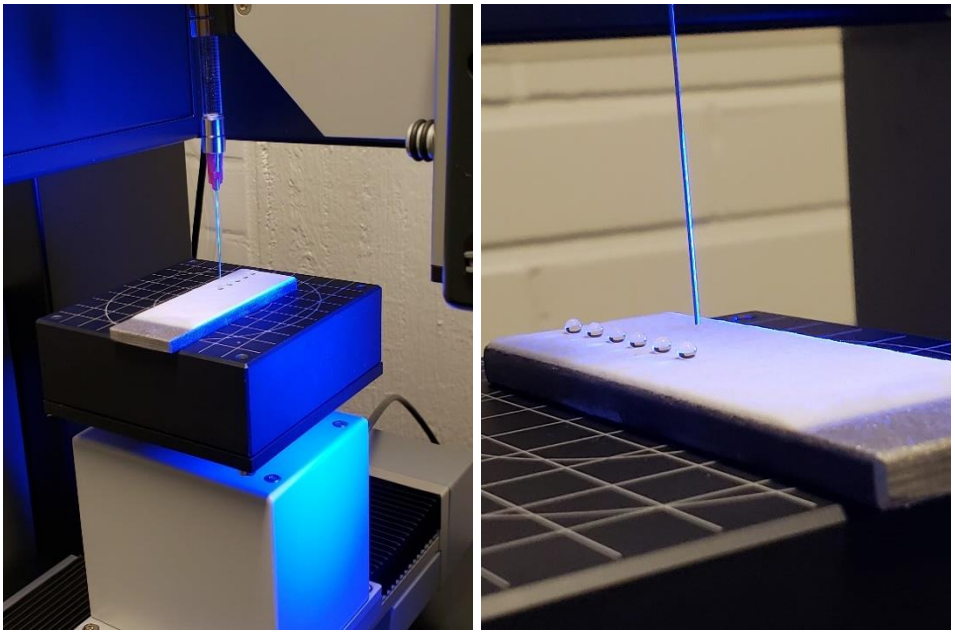

Figure 25. *Water droplets being released to the surface of oil-infused, cold sprayed coating during water contact angle measurements.*

5.4.3 Roughness by profilometer

Roughness of the sample coatings are measured with Alicona InfiniteFocus G5 profilometer (Austria) and data analysis is performed with IF-MeasureSuite program. Profilometric measurements were tested on 20x and 5x objectives. Objective selections (i.e. sample lengths) were made based on the recommended cut-off and elevation lengths (Table 1) according to Surface texture Geometrical Product Specifications (GPS) standard ISO 4288 (Ra range 10-80 µm → 8 mm cutoff and 40 mm elevation length).

Table 1. *The sampling length determined based on Ra and Rz (STN EN ISO 4288). Table adapted from Influence of Diverse Conditions during Accelerated Ageing of Beech Wood on its Surface Roughness* [86].

Average roughness, Ra (µm)	***Average height, Rz (µm)***	***Sampling length (mm)***	***Evaluation length (mm)***
(0.006) > Ra ≤0.02	(0.025) > Rz ≤ 0.1	0.08	0.4
0.02 > Ra ≤0.1	0.1> Rz ≤ 0.5	0.25	1.25
0.1 > Ra ≤2	0.5 > Rz ≤ 10	0.8	4
2 > Ra ≤10	10 > Rz ≤ 50	2.5	12.5
10 > Ra ≤80	50 > Rz ≤ 200	8	40

5.4.4 Oil stability by centrifuge

The samples are infused with lubricating liquid (Dupont Krytox GPL105, United States) before undergoing stability testing. The purpose of this test is to determine the amount of oil that remains held in the porous structure after the structure is rotated in a centrifuge. Weight measurements are taken before oil-infusion, after oil-infusion and after undergoing a centrifuge test using IEC CENTRA-7R (Finland). The samples are rotated in the centrifuge at 1000 RPM (revolution per minute) for 30 minutes at 25°C. The oil lockability of the samples is evaluated based on amount of oil lost (i.e. sample weights before and after stability testing). The data is reported in Table 7 of Results and Analysis.

6. RESULTS AND ANAYSIS

The cold spraying parameters of successfully coated samples are shown in Table 2. In total, seven high pressure (HP) coated samples and one low pressure (LP) sample are selected for testing and analysis.

Table 2. *Spraying parameters for successfully cold sprayed samples.*

Selected Samples	**2 (LP)**	**21 (HP)**	**22 (HP)**	**23 (HP)**	**24 (HP)**	**30 (HP)**	**33 (HP)**	**34 (HP)**
Polymer	PP	PP	PP	PP	PP	HDPE	PP-PPA (2:1)	PP-PPA-LDPE (2:1:1)
Gas Pressure (bar)	4,2	15	15	15	15	10	15	15
Gas Temp. (°C)	224	150	150	150	150	150	150	150
Powder feeding (RPM)	3,5	4	4	4	4	4	4	4
Substrate Temp. (°C)	120	135	135	135	135	135	135	135
Spraying Speed (m/min)	NA	10	10	10	10	5	10	10
Spray distance (mm)	15	40	50	60	60	40	40	40
Spray angle (°)	90	90	90	90	30	90	90	90
Number of passes	1	3	3	3	3	3	3	3

Sample 21, 22, 23 and 24 obtained sufficiently durable coat structure for sample preperation. Consequently, structure by microscope and oil stability testing was possible. Other sample coatings could not undergo sample preperation due to fragile coat structures. Additionally, measurement of roughness by profilometer could not be conducted for all oil-infused samples due to transparent oil affecting measurements. Testing for the samples listed in Table 2 is conducted as shown in Table 3:

Table 3. *Testing conducted for samples*

Test	Tested Samples
Structure by microscope	21, 22, 23, and 24 (non-infused)
Hydrophobicity by WCA	2 (oil infused), 21, 22, 23 & 24 (oil infused and non-infused), 30, 33 & 34 (oil infused)
Roughness by profilometer	2 (non-infused), 21, 22, 23 & 24 (oil infused and non-infused), 30, 33 & 34 (oil infused)
Oil stability by centrifuge	21, 22, 23 and 24 (oil infused)

Figure 26 shows an image of the coatings produced on samples 21, 22, 23 and 24. Although the coatings seem similar, they inhibit different structures and surface properties that are produced by the different spraying parameters.

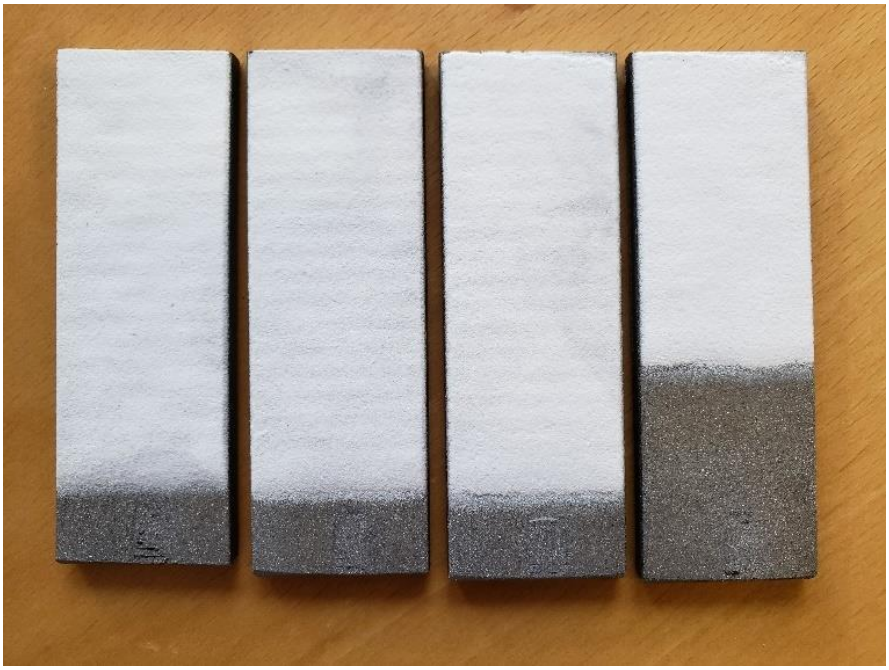

Figure 26. *Produced samples 21, 21, 23, 24 (left to right).*

6.1 Coating structure

Table 4 lists information obtained from images taken by the microscope. Figures 27 through 34 shows 5x and 10x images for the samples listed in Table 4.

Table 4. *Data obtained from structure.*

Speci-men	Average Coat thickness (µm)	Thickness STDV (µm)	Average Pore size (µm)	Pore size STDV (µm)
21	657.5	25,4	39.9	10,6
22	648.2	19,5	40.7	14,5
23	594.4	13,3	68.4	9,91
24	475.0	21,2	46.7	19,8

As shown in Table 4, the different samples obtained different thicknesses and pore sizes. As shown the differences between the samples are small.

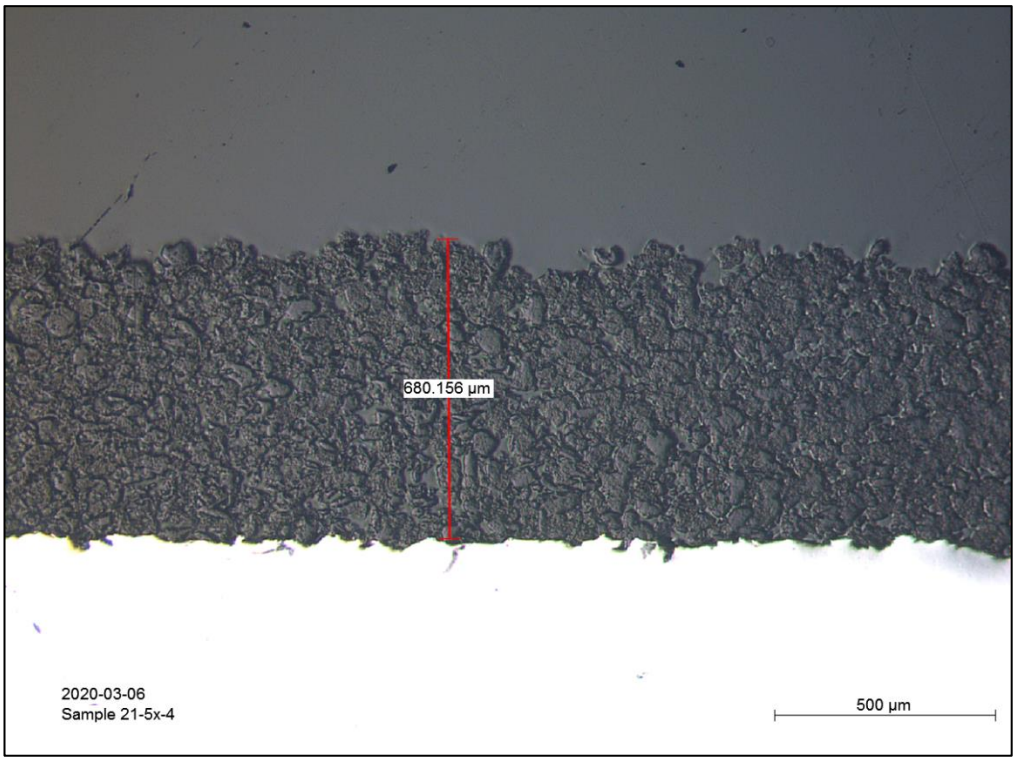

Figure 27. *Sample 21 microscope image (cross section)*

Figure 28 describes the microscopic image for sample 21 at 10x lens from a cross sectional view. The red arrows show the different components of the prepared sample: the coating structure, the micropores in the structure, the steel substrate and resin.

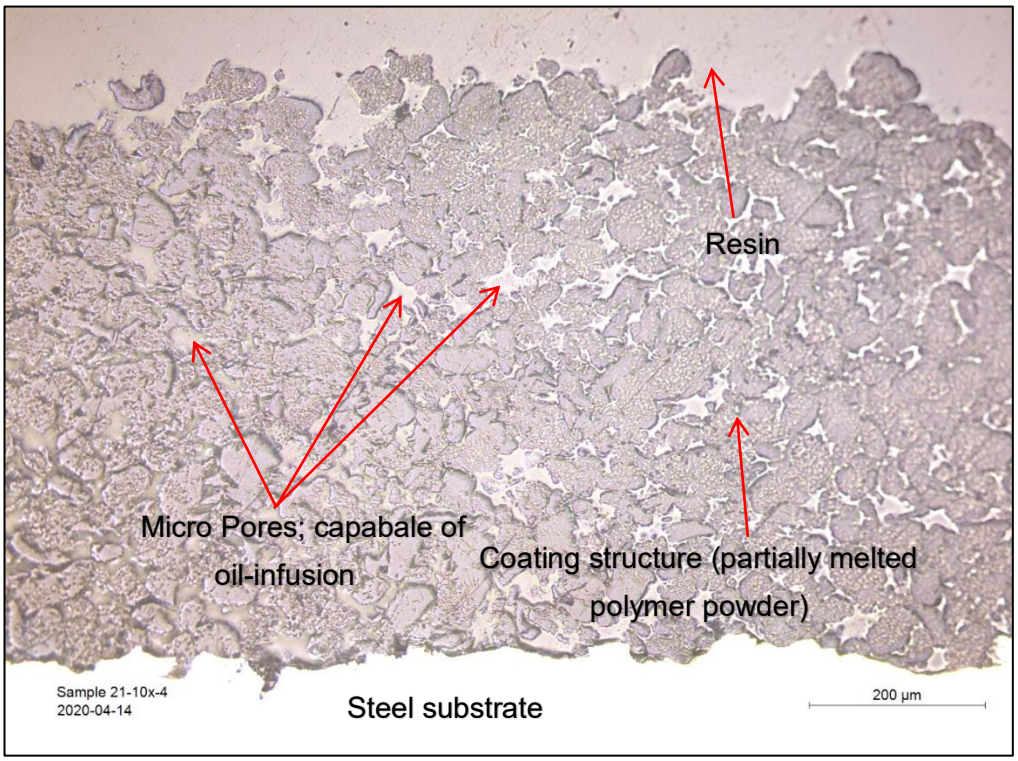

Figure 28. *Sample 21 (10x, cross section)*

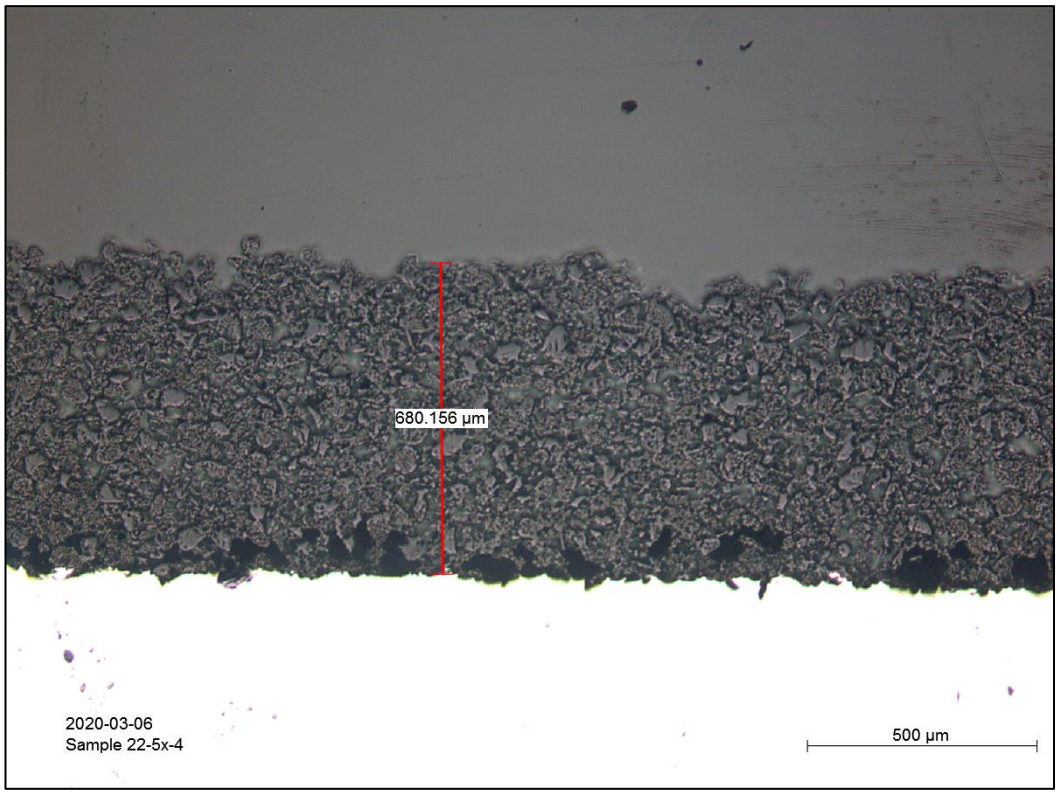

Figure 29. *Sample 22 microscope image (cross section)*

As shown in the microscopic images, the structure is highly porous due to the partial melting of the particle. This porous structure is desired for designing SLIPS.

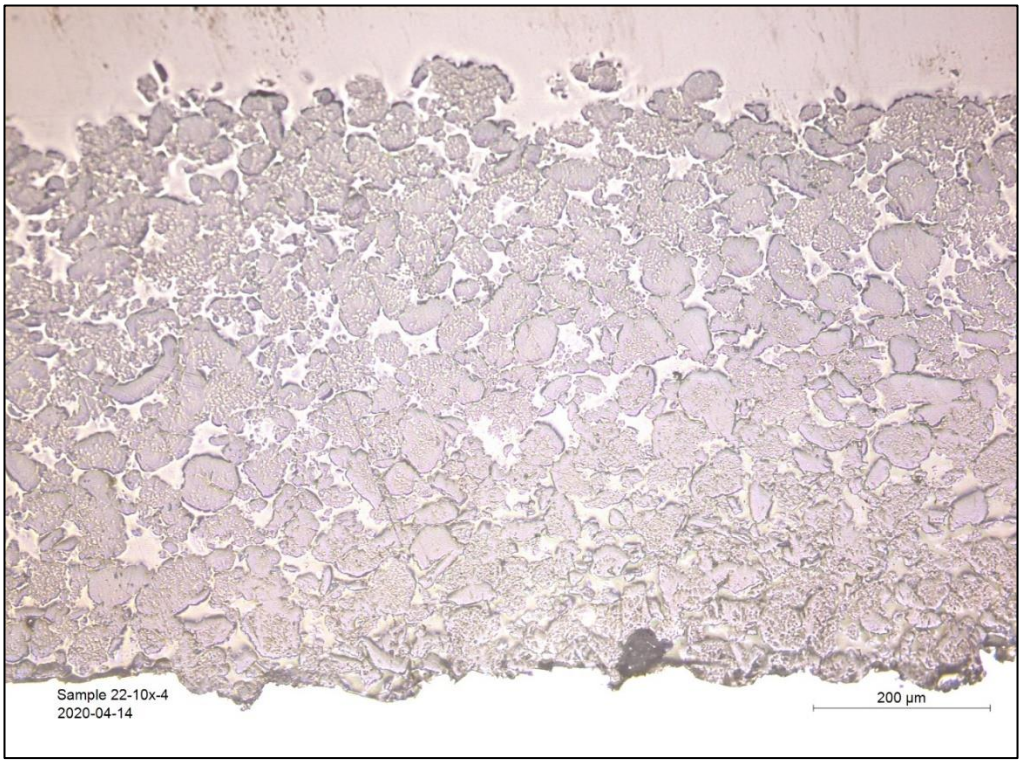

Figure 30. *Sample 22 (10x, cross section)*

Figures 31 and 32 are microscopic images for sample 23, which had the largest pore size. Although pore size is desired in SLIPS and that the cold spraying process helps with obtaining these pores, it is possible that oil stability is affected by pore size.

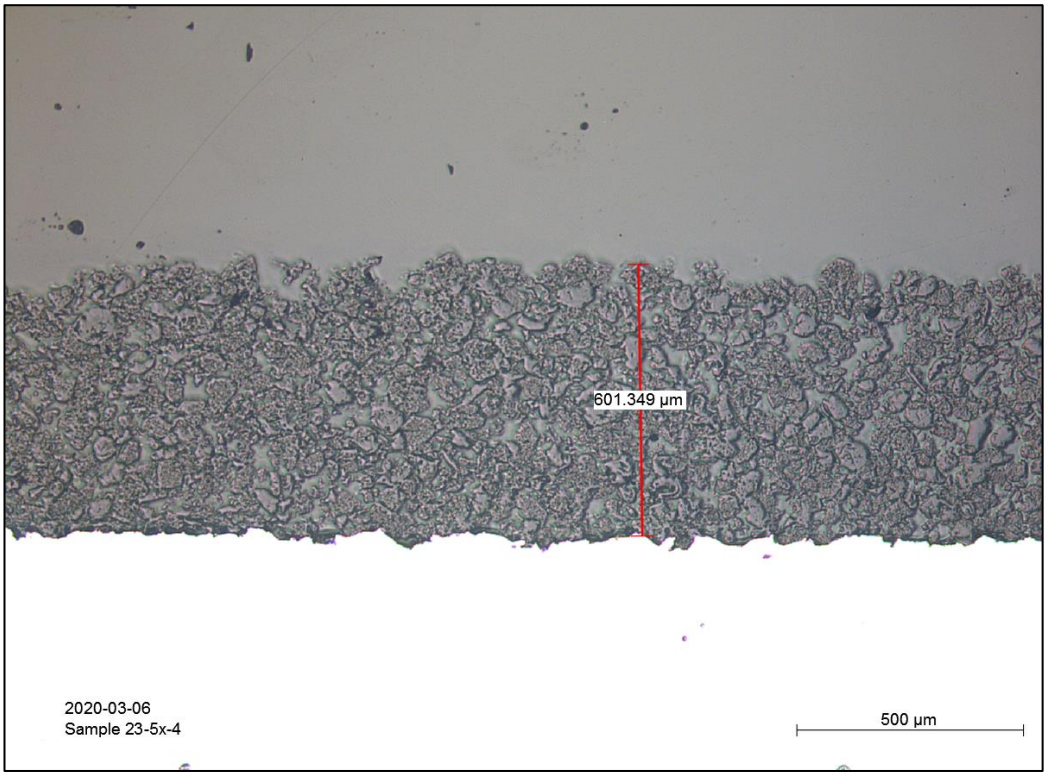

Figure 31. *Sample 23 microscope image (cross section)*

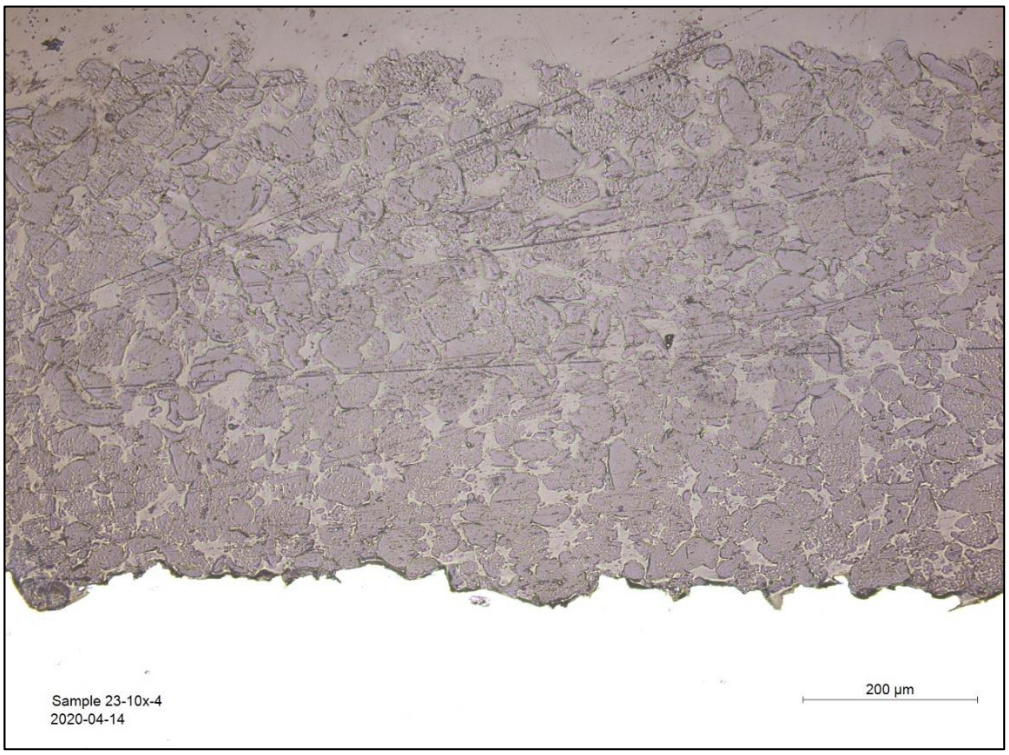

Figure 32. *Sample 23 (10x, cross section)*

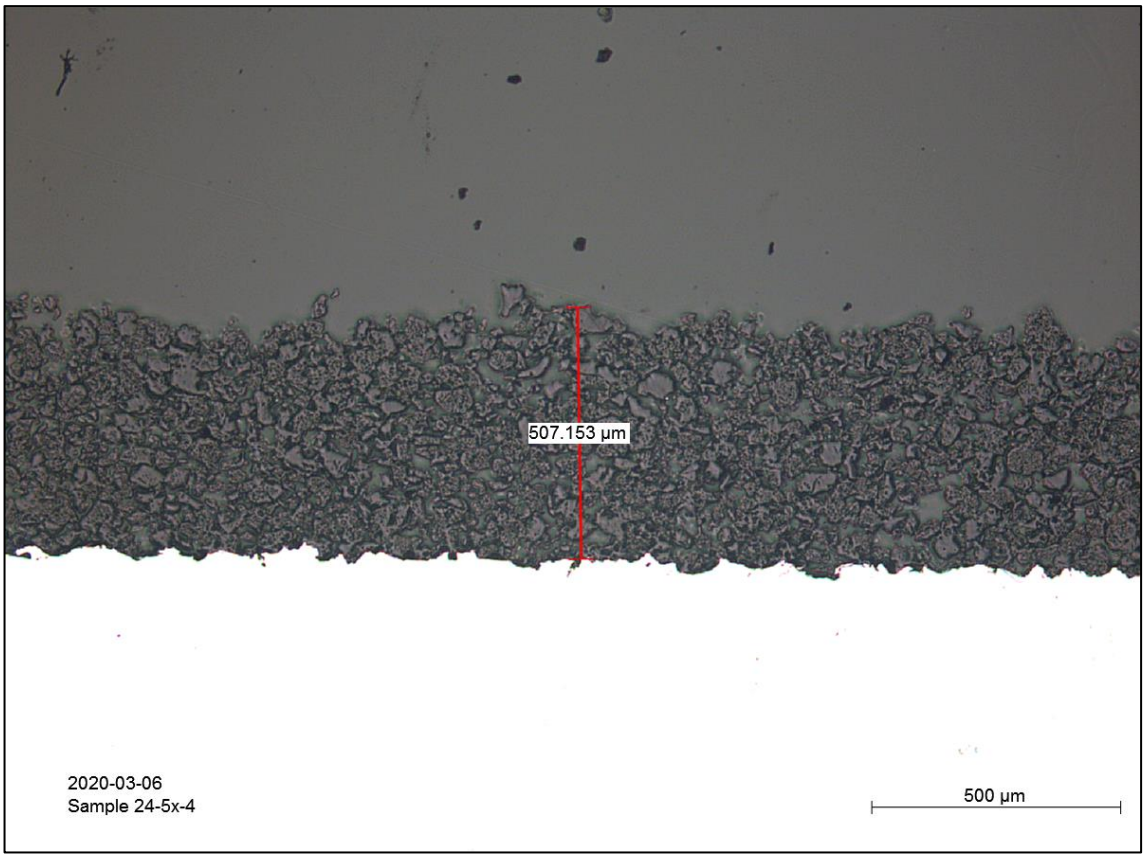

Figure 33. *Sample 24 microscope image (cross section)*

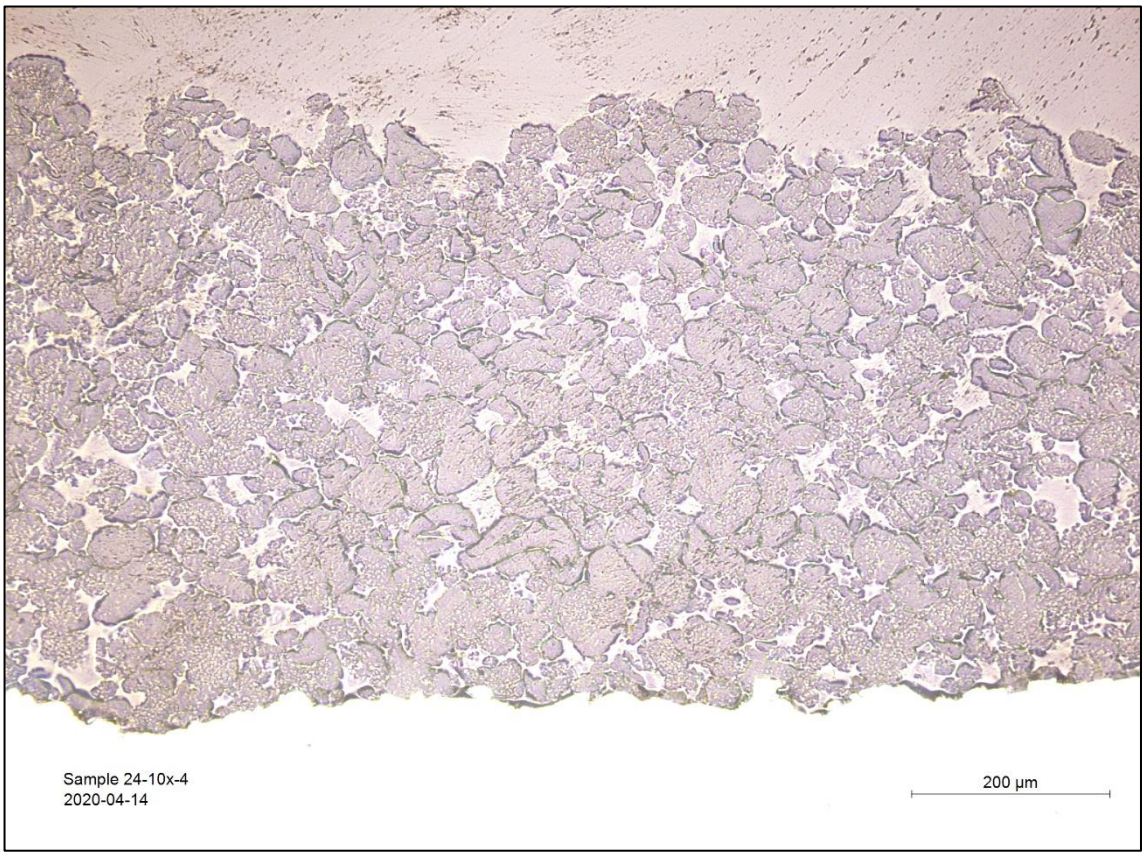

Figure 34. *Sample 24 (10x, cross section)*

6.2 Water contact angle (WCA)

Table 5 shows the contact angles for different samples. All samples showed WCA greater than 90°. Additionally, non-infused samples 22 and 23 show water contact angles greater than 150°. Conventionally, WCA is measured for a water droplet that is balanced on a surface with two interfaces 1) a solid and 2) the surrounding atmosphere (air).

Table 5. *WCA measurements*

Sample	Liquid Drop	CA(m) [°]	StDev [°]
2, oil-infused	Water	94,61	9,49
21, unoiled	Water	149,79	1,02
21, oil-infused	Water	135,11	3
22, unoiled	Water	150,62	3,51
22, oil-infused	Water	135,17	2,49
23, unoiled	Water	151,46	1,75
23, oil-infused	Water	135,13	2,21
24, unoiled	Water	144,02	1,48
24, oil-infused	Water	118,54	5,34
30, oil-infused	Water	110,38	15,12
33, oil-infused	Water	108,74	3,93
34, oil-infused	Water	102,2	3,33

For the oil infused samples, a third interface (i.e. the oil) is introduced. In other words, the outer edge of the water droplet on the oil-infused surface is touching three interfaces: 1) the solid, 2) the surrounding air, and 3) the oil or the second liquid. Therefore, the measured is the "apparent" WCA. There exists models for interpretting WCA on liquid-infused surfaces. An example model for the "apparent" WCA on oil-infused surfaces and accounting of the affect of oil is described in Figure 35.

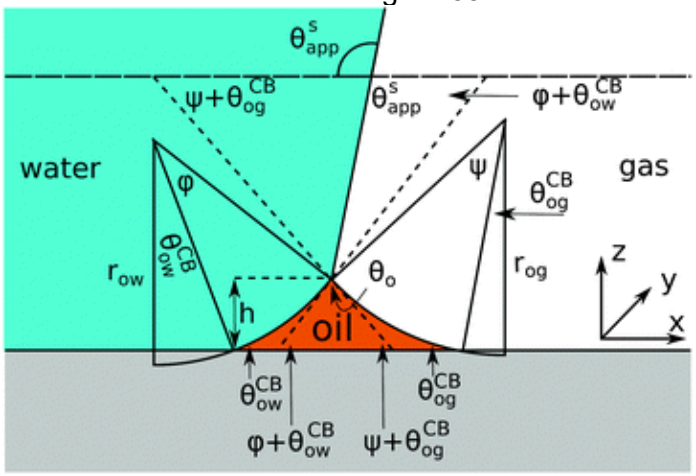

Figure 35. *A model for intepretting apparent WCA of oil infused surfaces* [87].

Figure 36 compares the measured WCA for oil-infused and non-infused samples 21, 21, 23, 24. Comparison between the real wetting behavior of the non-infused (two interfacial tensions) sample and oil-infused (three interfacial tensions) samples is beyond the scope of this thesis because it is not relevant for evaluation of the icephobic behavior.

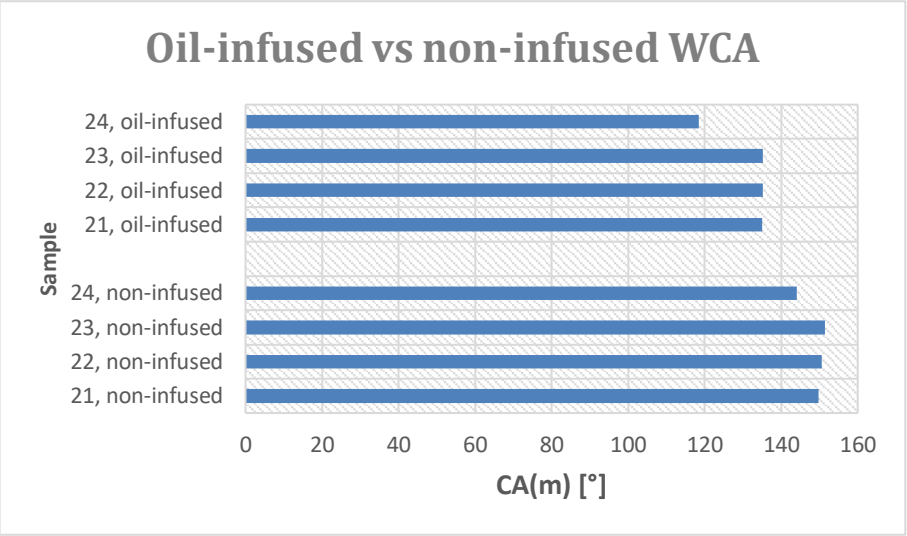

Figure 36. *WCA comparision for oil-infused vs non-infused samples*

6.3 Surface roughness and topography

Table 6 shows roughness measurements by profilometer. These measurements could not be conducted for all oiled samples due to transparent oil.

Table 6. *Roughness measurements.*

Sample	Ra, Ave rough-ness (µm)	Sa, mean peak to valley height (µm)	Rz, average height (µm)	Sz, maximum height (µm)
2	28	30	191	294
21	18	18	120	197
21oil	23	25	171	270
22	20	21	136	236
22oil	31	31	229	348
23	21	21	152	285
23oil	27	29	218	306
24	21	22	135	219
24oil	30	29	220	307
30oil	16	24	108	192
33oil	17	21	118	227
34oil	25	27	193	227

Figure 37 compares roughness measurements for oil-infused and non-infused samples that have similar structures and spraying parameters.

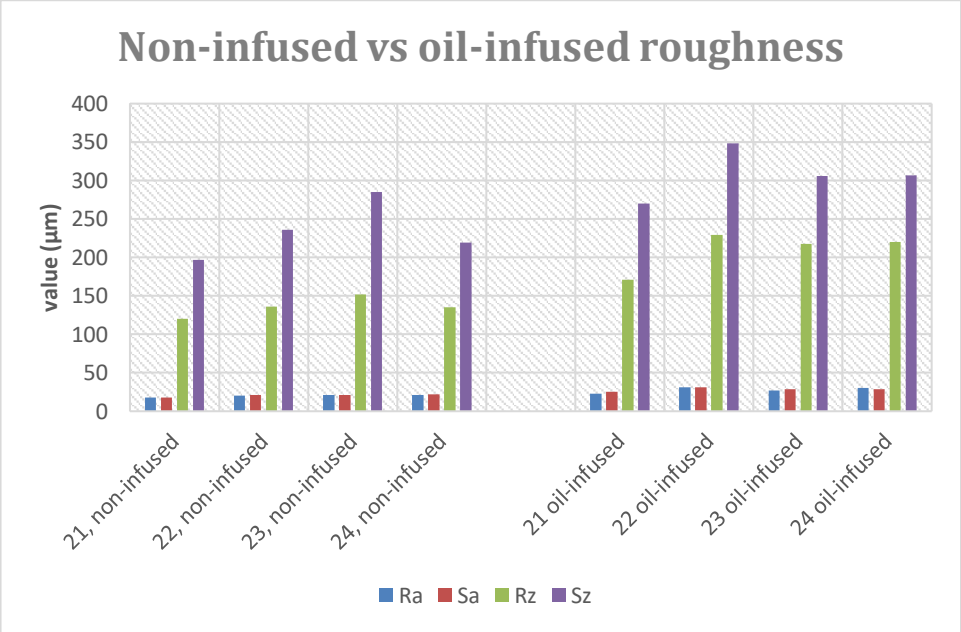

***Figure 37**. Roughness conmparison of oil-infused vs non-infused samples*

As shown in Figure 37, oil-infused surfaces behave differently than non-infused surfaces. The roughness of the oil-infused is greater than the non-infused samples, which is counterintuitive. It is possible that the reliability of roughness measurement is in question due to oil transparent samples affecting the measurements, which are obtained using a camera. Either way, oil infusion is an important step in designing SLIPS as shown by the results. Also, the oil behavior at freezing temperature could be very significant.

6.3.1 Surface topography

Figures 38 through Figure 45 show the topography for samples as listed in Table 3. Surfaces topography allows for a visual analysis for the behavior of oil on the surfaces. It is shown that the surface topography of the surfaces is very similar, with the exception of the height of surface aspirities. From this point, the effect of the spraying parameters on surface and structural properties (and thus surface behavior) is very small for surfaces sprayed with the same method but different parameters. Thus, the spraying parameters are negligible for optimizing SLIPS surface behavior which are important for this study (i.e. icephobicity and icephobic behavior of the surfaces). Optimizing spraying parameters can be the final step for studying icephobic behavior of different surfaces. Even for samples sprayed with different cold spray guns (low pressure and high pressure), the surface aspirities seem to be similar. Sample 2 shown below is produced

with low pressure spray gun, while sample 21 is produced with a high pressure spray gun. Overall, the surface aspirities look similar but have different heights (i.e. roughnesses). Nevertheless, the samples will have slightly different surface properties.

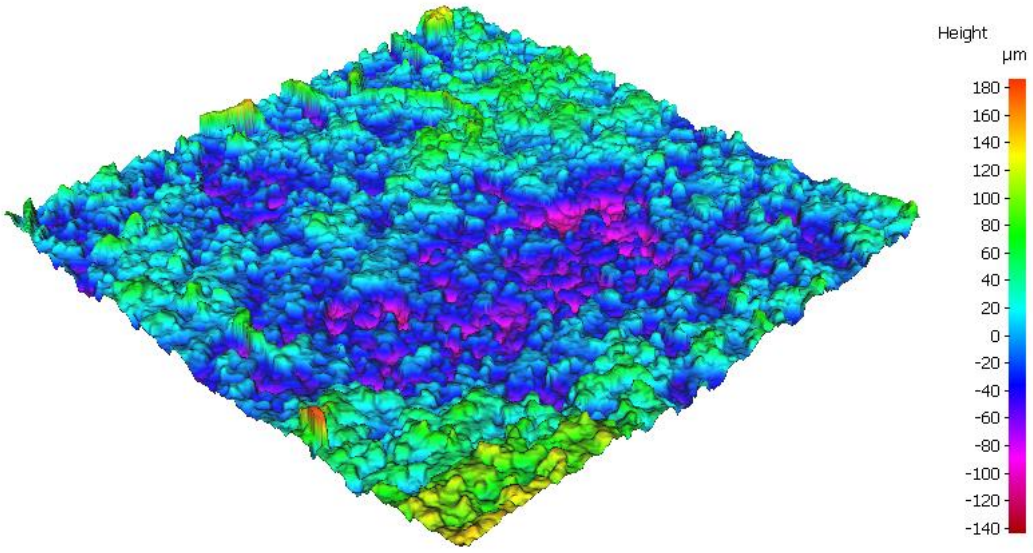

Figure 38. *Sample 2, surface topography*

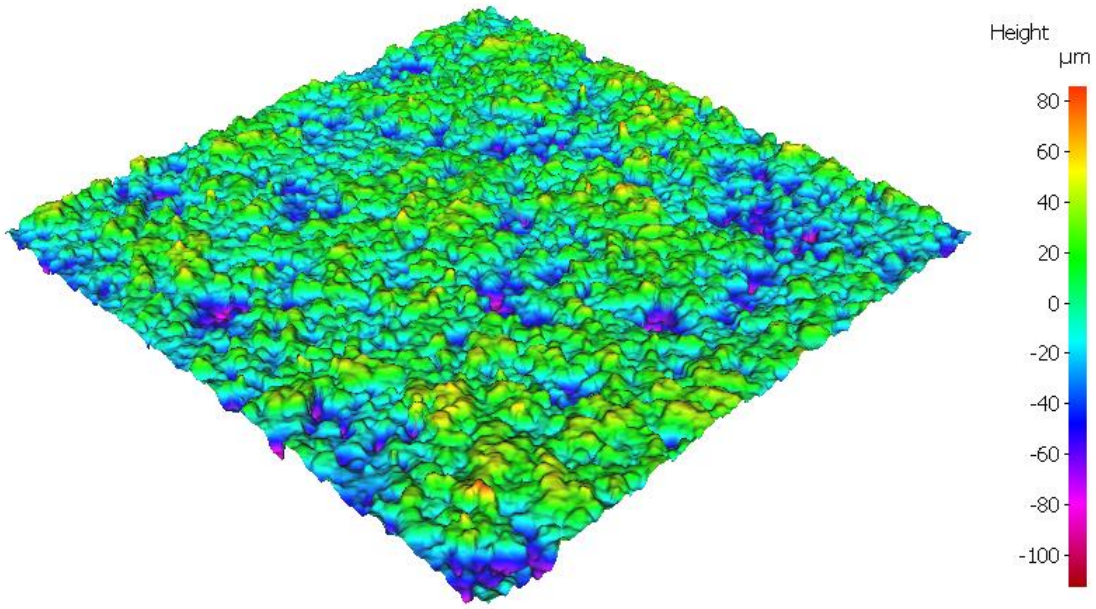

Figure 39. *Sample 21, surface topography*

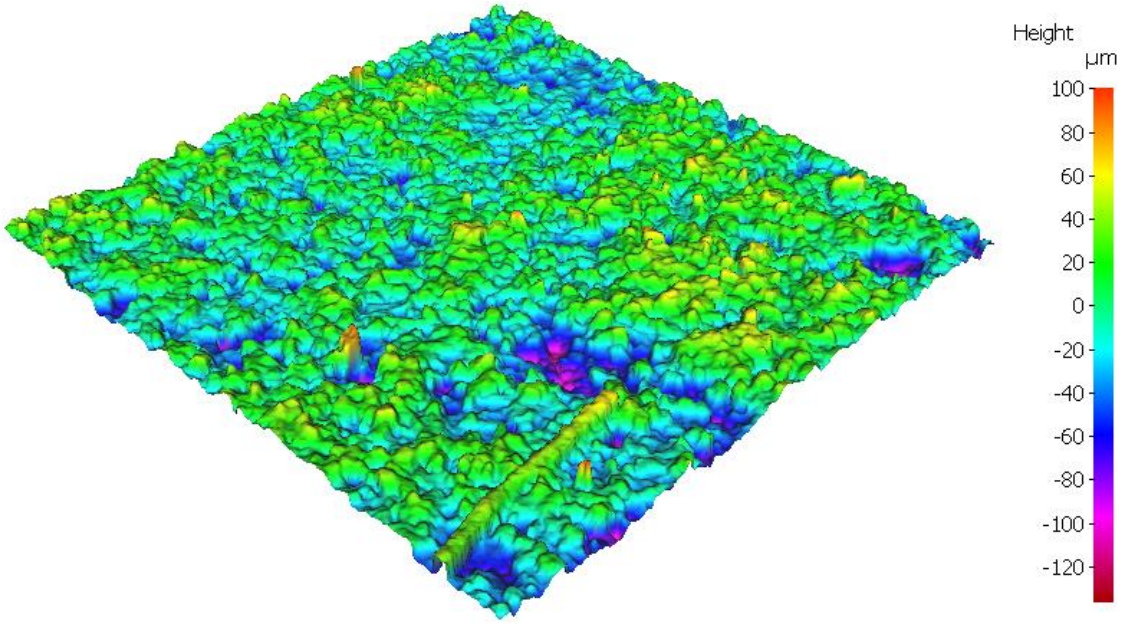

Figure 40. *Sample 22, surface topography*

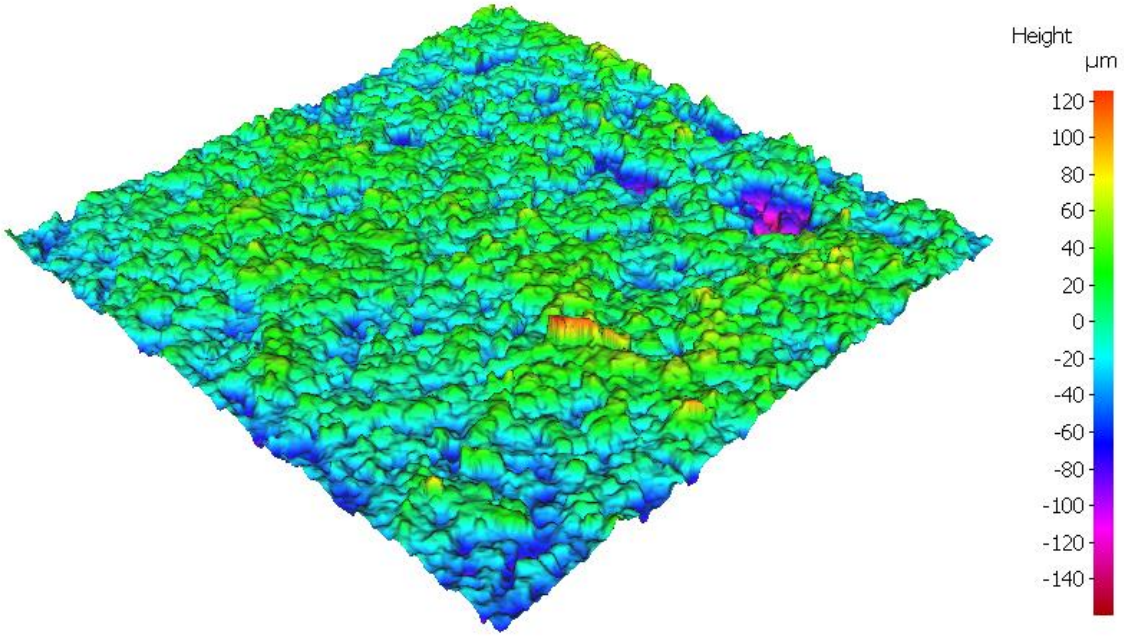

Figure 41. *Sample 23, surface topography*

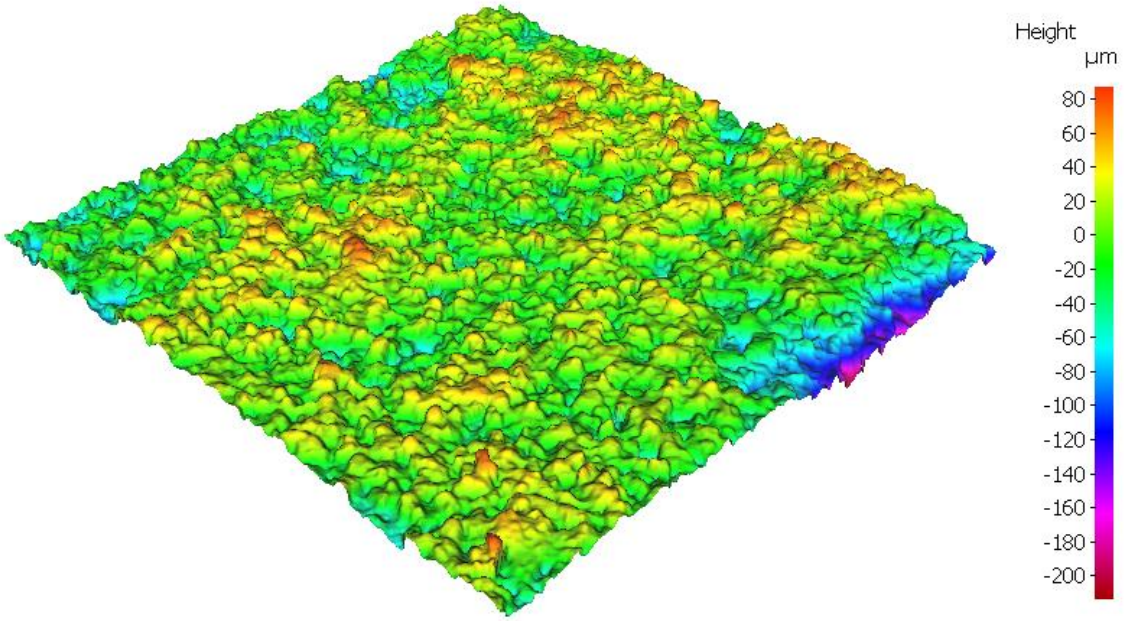

Figure 42. *Sample 24, surface topography*

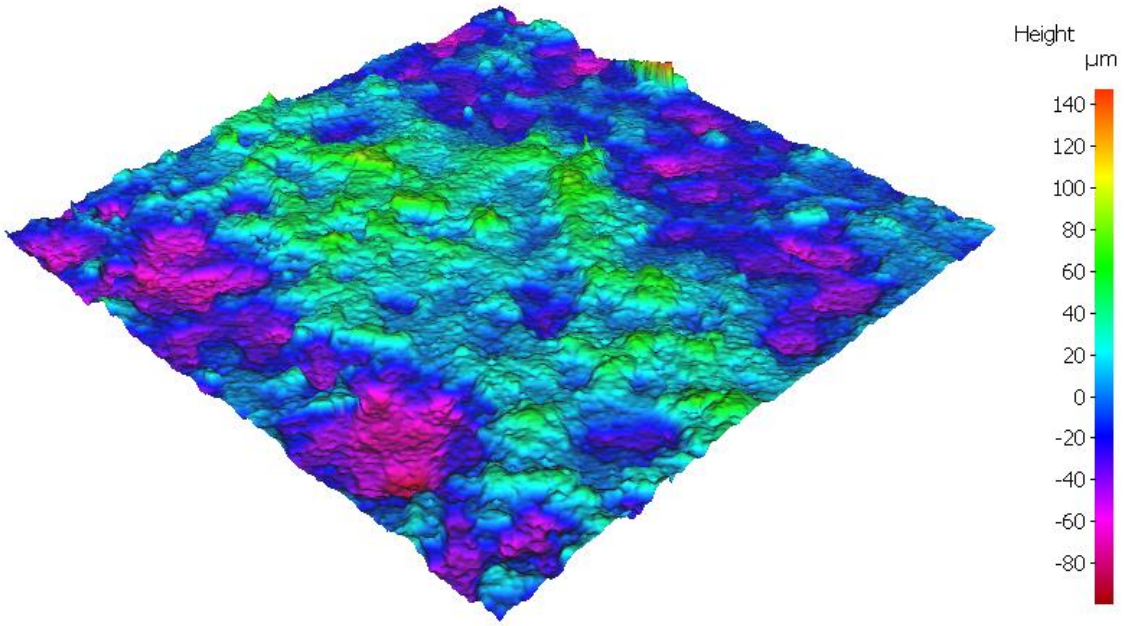

Figure 43. *Sample 30, surface topography*

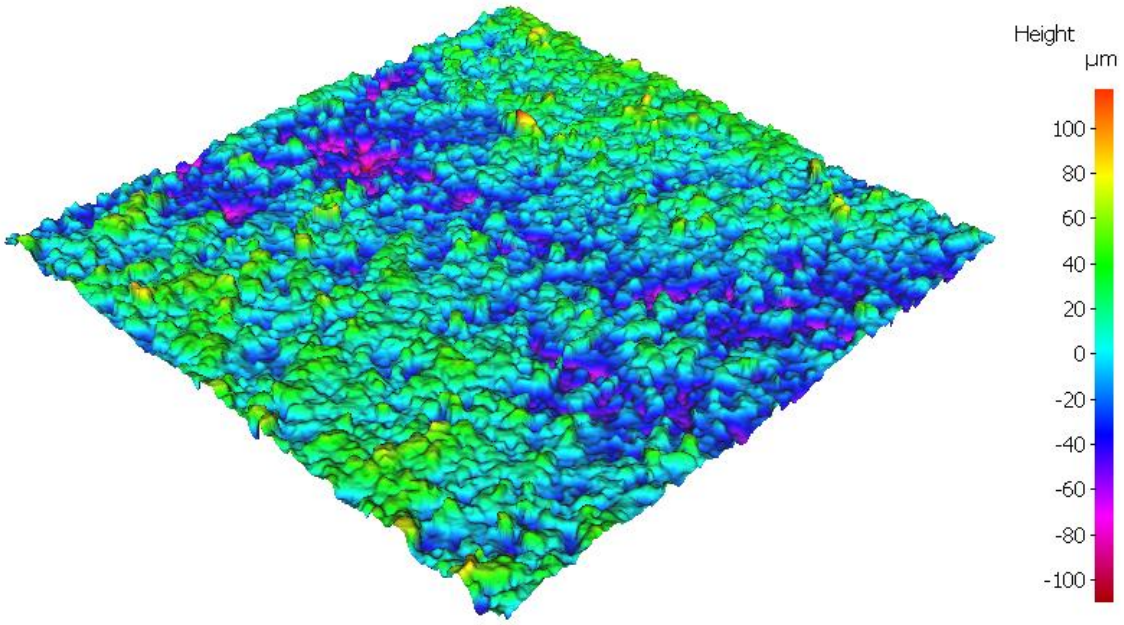

Figure 44. *Sample 33, surface topography*

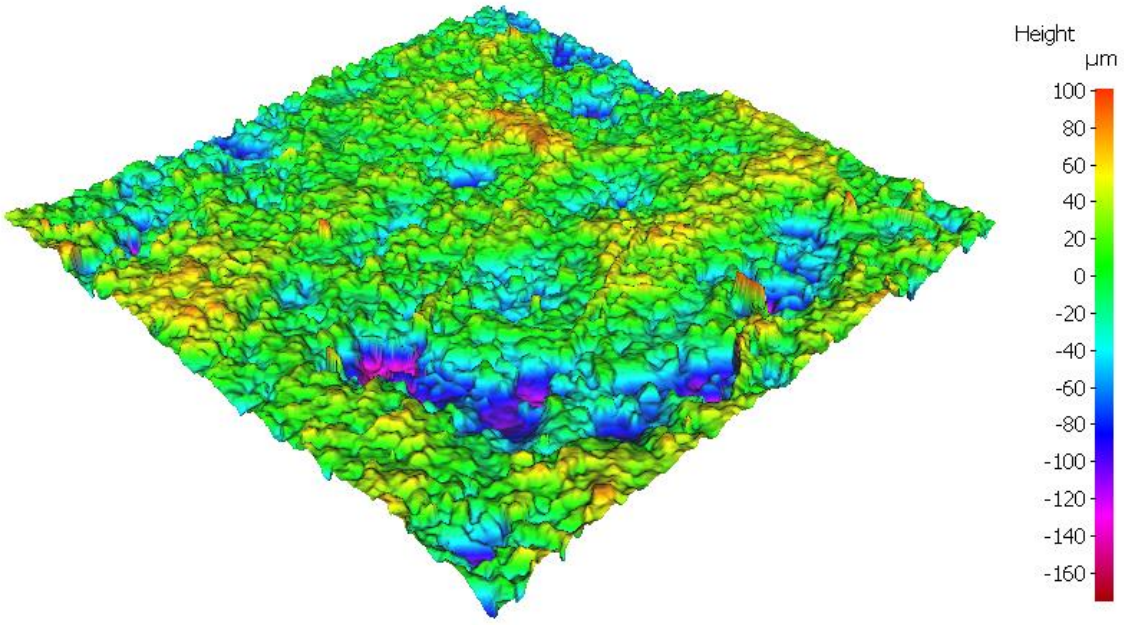

Figure 45. *Sample 34, surface topography*

6.3.2 Spray distance vs. roughness

Figure 46 plot shows that as spraying distance increases, surface roughness increases. This finding is consistent with another cold spraying study [88] in a different area.

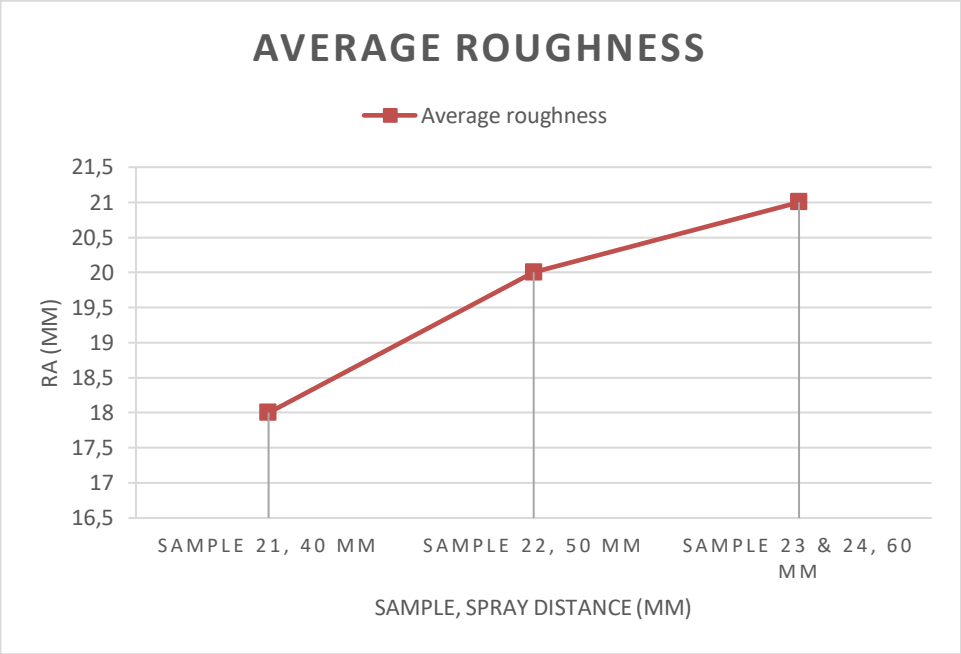

Figure 46. *Spray distance vs average roughness*

6.4 Oil Stability of SLIPS

The purpose of this test is to evaluate the amount of oil the structure can hold while the samples are in a centrifuge. In other words, it is to measure the oil stability of SLIPS. Table 7 and Figure 47 show the amount of oil infused in the samples verses the amount of oil loss in grams for successful samples 21, 22, 23 and 24.

Table 7. *Oil stability data.*

Sample	Coat area (cm^2)	Sample weight (g)	Weight after oil infusion (g)	Weight after centrifuge test (g)	Oil lockability (%)
21	13x17.5	106,1	107,1	107,1	100
22	13x17.5	107,3	108,3	108,2	90,0
23	13x17.5	107,4	108,4	108,3	90,0
24	13x15.3	108,4	109,3	109,0	90,0

Figure 47 shows the amount of oil infused in the samples (blue bars) verses how much oil is lost (red bars) for samples 21, 22, 23 and 24. The SLIPS design relies on a porous

structure, and as implied in the name should have the capacity to be infused with a lubricating liquid that remains held in its porous structure. With cold spraying, the coating is composed of “unmelted” or partially melted polymer particles, that is, the structure which is capable of functional oil infusion. All samples achieved high, and in some cases perfect, oil stability which is a desired behavior of cold sprayed SLIPS coatings.

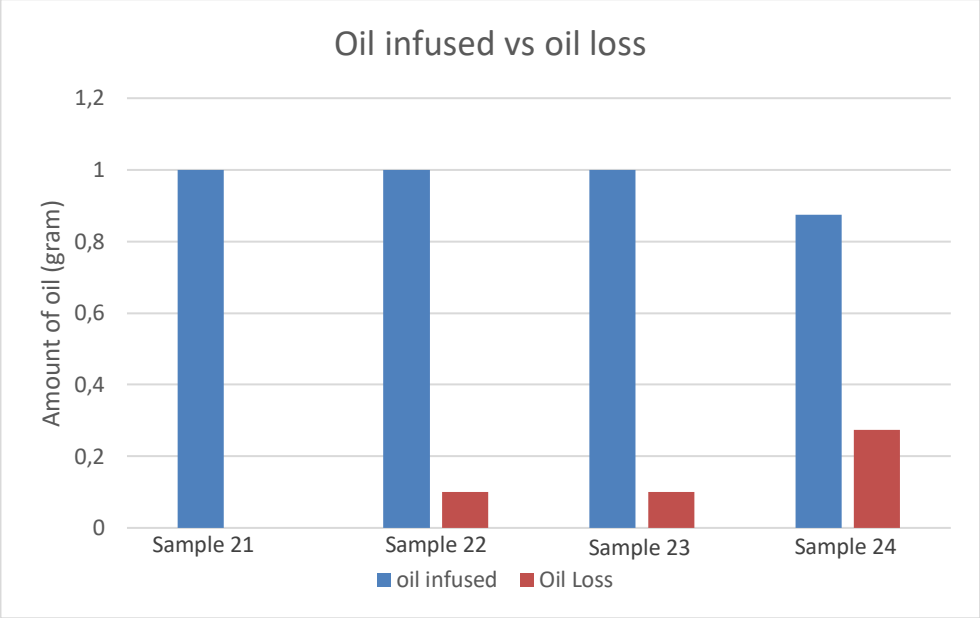

Figure 47. *Oil infused (blue bars) vs oil lost (red bar). It can be observed that there was no oil loss for Sample 21.*

Sample 21 with the smallest pore size, obtained the best oil stability with no oil leaving the sample structure. Although large pore size was desired for this study, it is obvious that structures having larger pore sizes have reduced oil stability.

Nevertheless, the results from this test are preliminary: further testing can be performed such that greater rotational speed is used and more differences between the samples is observed. For future studies involving specific applications (e.g. airplanes), the rotational speed can be specified based on those applications. For example, the speed of the centrifuge can be calculated based on an airplane speed. However, the behavior of the oil in application-specific conditions must be considered (i.e. in freezing conditions).

7. DISCUSSION

Ice accretion is a serious problem that requires the development of icephobic surfaces. Since the 1930s, studies attempted to produce successful icephobic surfaces by selecting highly hydrophobic surfaces and surfaces that have low ice adhesion strength values, as tested in icing wind tunnels. Despite the availability of very few products labeled "icephobic" on the market, there has been skepticism over their effectiveness. The inability to produce successful icephobic surfaces can primarily be attributed to poor understanding of ice formation, weak connection to wettability, unreliability of icing wind tunnel testing and other factors including experimental biases in icephobics research.

It has been established that the nature-inspired SLIPS inhibit highly hydrophobic properties and nature-mimicking behaviors (i.e. lotus leaf). It has been hypothesized that SLIPS can be used as icephobic surfaces based on low ice adhesion strength of commercially tested SLIPS [30] at Tampere University. Production of SLIPS using thermal spray technology has been attempted at Tampere University using flame spraying [34] , however cold spraying of polymers (and thus, the production of SLIPS using cold spraying technology) was unexplored. This study demonstrated that the production of cold sprayed SLIPS with polymers is achievable due the partial melting of powder upon impact with the substrate, resulting in a porous structure that is capable of oil infusion.

Conventionally, SLIPS design is challenging due to complicated surface preparation and poor oil stability. Cold spraying is advantageous over other SLIPS design methods because it does not require complicated surface preparation and has excellent oil stability, as demonstrated in this study. These findings are exciting, especially as cold spraying is a becoming part of cutting-edge fields. Although the production of SLIPS using cold spraying is achievable, the range of surface properties possibly obtained by varying cold spraying parameters is small. However, the SLIPS design method (i.e. oil infusion, powder selection, etc) may results in a wider range of properties and surface behaviors.

The SLIPS produced in this study inhibit high WCA and may also possess low ice adhesion strength against some surfaces, based on previous ice adhesion of tested commercial SLIPS [30]. Due to limited understanding of ice formation, unreliability of icing wind tunnel testing, and impossibility to compare ice adhesion data, the author of this study cannot conclude that SLIPS produced in this study are icephobic based on a general definition of the term and limited knowledge about behavior of these surfaces in real conditions. However, further testing is still encouraged in future icephobics studies.

8. CONCLUSION

This study showed that the production of cold sprayed SLIPS is feasible. The cold spraying process helps in producing porous coating structures due to the partial melting of the sprayed powder particles, which aids with the production of SLIPS. Currently, cold sprayed SLIPS coatings may be used in icephobics studies based on debated connection with wettability or by using current testing methods such as ice wind tunnels however, drawn conclusions about icephobic behavior of the produced surfaces and structures should be carefully analyzed with thorough understanding about ice formation and consideration to other studies.

REFERENCES

[1] Yirtici O, Tuncer IH, Ozgen S. Ice accretion prediction on wind turbines and consequent power losses. *J Phys : Conf Ser*. 2016;753:022022. https://doi.org/10.1088%2F1742-6596%2F753%2F2%2F022022. Accessed Feb 7, 2020. doi: 10.1088/1742-6596/753/2/022022.

[2] Why ice and airplanes don't mix. https://www.bjtonline.com/business-jet-news/why-ice-and-airplanes-dont-mix. Updated 2014. Accessed Mar 3, 2020.

[3] Figure 2: Ice accretion on a vessel (kubat & timco, 2005). https://www.researchgate.net/figure/Ice-accretion-on-a-Vessel-Kubat-Timco-2005_fig2_311250687. Accessed Mar 3, 2020.

[4] Ice covered communication equipment by jose azel. https://fineartamerica.com/featured/ice-covered-communication-equipment-jose-azel.html. Accessed Mar 10, 2020.

[5] Detecting ice on wind-turbine blades. https://www.windpowerengineering.com/detecting-ice-on-wind-turbine-blades/. Accessed Mar 10, 2020.

[6] SKYbrary. In-flight icing - SKYbrary aviation safety. https://www.skybrary.aero/index.php/In-Flight_Icing. Updated 20192020.

[7] Xiao Huang, Nick Tepylo, Valérie Pommier-Budinger, Marc Budinger, Elmar Bonaccurso, Philippe Villedieu, Lokman Bennani. A survey of icephobic coatings and their potential use in
a hybrid coating/active ice protection system for
aerospace applications. . 2019.

[8] De-icing. . 2020. https://en.wikipedia.org/w/index.php?title=De-icing&oldid=937510303. Accessed Mar 3, 2020.

[9] Duffell A. Does ice or snow affect railroads? . . 2018.

[10] Lockney D. Anti-icing formulas prevent train delays . https://spinoff.nasa.gov/Spinoff2012/t_1.html. Updated 20122020.

[11] Brassard J, Laforte C, Guérin F, Blackburn C. Icephobicity: Definition and measurement regarding atmospheric icing. In: ; 2017. Accessed Feb 10, 2020.

[12] History of aircraft deicing . . . https://www.copybook.com/companies/kilfrost/history-of-kilfrost-gallery/history-of-aircraft-deicing-01.

[13] NA. What is anti-icing? | cargill. https://www.cargill.com/what-is-anti-icing. Updated 20202020.

[14] Parent O, Ilinca A. Anti-icing and de-icing techniques for wind turbines: Critical review. *Cold Regions Science and Technology*. 2011;65(1):88-96. http://www.sciencedirect.com/science/article/pii/S0165232X10000108. Accessed Apr 24, 2020. doi: 10.1016/j.coldregions.2010.01.005.

[15] Phobia | meaning of phobia by lexico. https://www.lexico.com/definition/phobia. Accessed Feb 7, 2020.

[16] Marmur A. Super-hydrophobicity fundamentals: Implications to biofouling prevention. *Biofouling*. 2006;22(2):107-115. https://doi.org/10.1080/08927010600562328. Accessed May 20, 2020. doi: 10.1080/08927010600562328.

[17] Appendix C: Contact angle goniometry. In: *Surface design: Applications in bioscience and nanotechnology*. John Wiley & Sons, Ltd; 2009:471-473. https://onlinelibrary.wiley.com/doi/abs/10.1002/9783527628599.app3. Accessed Apr 6, 2020.

[18] Korhonen JT, Huhtamäki T, Ikkala O, Ras RHA. Reliable measurement of the receding contact angle. *Langmuir*. 2013;29(12):3858-3863. https://doi.org/10.1021/la400009m. Accessed May 20, 2020. doi: 10.1021/la400009m.

[19] Taheri-Kafrani A, Shirzadfar H, Tavassoli-Kafrani E. Chapter 5 - dendrimers and dendrimers-grafted superparamagnetic iron oxide nanoparticles: Synthesis, characterization, functionalization, and biological applications in drug delivery systems. In: Grumezescu AM, ed. *Nano- and microscale drug delivery systems*. Elsevier; 2017:75-94. http://www.sciencedirect.com/science/article/pii/B9780323527279000054. Accessed Feb 20, 2020.

[20] Stenroos C. Properties of icephobic surfaces in different icing conditions. . 2015. https://www.openaire.eu/search/publication?articleId=od_____1073::31c5c167801d8d1632826c25a34e5841.

[21] Wu X, Silberschmidt VV, Hu Z, Chen Z. Surface & coatings technology. *Surface & coatings technology*. 1986;358:207-214. http://www.sciencedirect.com/science/article/pii/S0257897218312490.

[22] NEWBLOOM GM, THOMPSON WA, FRONING MJ, GHABCHI A. Thermal spray for durable and large-area hydrophobic and superhydrophobiciicephobic coatings. . 2016.

[23] Hejazi V, Sobolev K, Nosonovsky M. From superhydrophobicity to icephobicity: Forces and interaction analysis. *Scientific reports*. 2013;3(1):2194. https://www.ncbi.nlm.nih.gov/pubmed/23846773. doi: 10.1038/srep02194.

[24] Ta VD, Dunn A, Wasley TJ, et al. Laser textured superhydrophobic surfaces and their applications for homogeneous spot deposition. *Applied Surface Science*.

2016;365:153-159. http://dx.doi.org/10.1016/j.apsusc.2016.01.019. doi: 10.1016/j.apsusc.2016.01.019.

[25] HENNA NIEMELÄ-ANTTONEN. *Wettability and anti-icing properties of slippery liquid infused porous surfaces.* Tampere University of Technology; 2015.

[26] Huang X, Tepylo N, Pommier-Budinger V, et al. A survey of icephobic coatings and their potential use in a hybrid coating/active ice protection system for aerospace applications. *Progress in Aerospace Sciences*. 2019;105:74-97. http://dx.doi.org/10.1016/j.paerosci.2019.01.002. doi: 10.1016/j.paerosci.2019.01.002.

[27] Andrew Hardesty Work Jr. *The measurement of the adhesion of glaze ice.* . University of Louisville.

[28] Work A, Lian Y. A critical review of the measurement of ice adhesion to solid substrates. *Progress in Aerospace Sciences*. 2018;98:1-26. http://dx.doi.org/10.1016/j.paerosci.2018.03.001. doi: 10.1016/j.paerosci.2018.03.001.

[29] Irajizad P, Nazifi S, Ghasemi H. Icephobic surfaces: Definition and figures of merit. *Advances in Colloid and Interface Science*. 2019;269:203-218. http://www.sciencedirect.com/science/article/pii/S0001868618303312. Accessed May 8, 2020. doi: 10.1016/j.cis.2019.04.005.

[30] CAMPICIANO G. Adesione del ghiaccio sulla superficie dei materiali esaminati e fattori che la influenzano. https://morethesis.unimore.it/theses/available/etd-03102018-124405/. Updated 2018. Accessed May 7, 2020.

[31] Koivuluoto H, Koivuluoto H, Stenroos C, et al. Anti-icing behavior of thermally sprayed polymer coatings. *J Therm Spray Tech*. 2017;26(1):150-160. doi: 10.1007/s11666-016-0501-x.

[32] Bharathidasan T, Kumar SV, Bobji MS, Chakradhar RPS, Basu BJ. Effect of wettability and surface roughness on ice-adhesion strength of hydrophilic, hydrophobic and superhydrophobic surfaces. *Applied Surface Science*. 2014;314:241-250. http://dx.doi.org/10.1016/j.apsusc.2014.06.101. doi: 10.1016/j.apsusc.2014.06.101.

[33] Fu Q, Wu X, Kumar D, et al. Development of Sol–Gel icephobic coatings: Effect of surface roughness and surface energy. *ACS Appl Mater Interfaces*. 2014;6(23):20685-20692. https://doi.org/10.1021/am504348x. Accessed Apr 8, 2020. doi: 10.1021/am504348x.

[34] Donadei V, Koivuluoto H, Sarlin E, Vuoristo P. Icephobic behaviour and thermal stability of flame-sprayed polyethylene coating: The effect of process parameters . *Journal of Thermal Spray Technology*. 2019(11 November 2019).

[35] Hassan MF, Lee HP, Lim SP. The variation of ice adhesion strength with substrate surface roughness. *Meas Sci Technol*. 2010;21(7):075701. https://doi.org/10.1088%2F0957-0233%2F21%2F7%2F075701. Accessed May 20, 2020. doi: 10.1088/0957-0233/21/7/075701.

[36] Laforte C. How a solid coating can reduce the adhesion of ice on a structure. *Academia*. . https://www.academia.edu/29500989/How_a_solid_coating_can_reduce_the_adhesion_of_ice_on_a_structure. Accessed May 20, 2020.

[37] Zou M, Beckford S, Wei R, Ellis C, Hatton G, Miller MA. Effects of surface roughness and energy on ice adhesion strength. *Applied Surface Science*. 2011;257(8):3786-3792. http://dx.doi.org/10.1016/j.apsusc.2010.11.149. doi: 10.1016/j.apsusc.2010.11.149.

[38] Fu Q, Wu X, Kumar D, et al. Development of Sol–Gel icephobic coatings: Effect of surface roughness and surface energy. *ACS Appl Mater Interfaces*. 2014;6(23):20685-

20692. https://doi.org/10.1021/am504348x. Accessed May 20, 2020. doi: 10.1021/am504348x.

[39] Simundić A. Bias in research. *Biochemia medica*. 2013;23(1):12-15. https://www.ncbi.nlm.nih.gov/pubmed/23457761. doi: 10.11613/BM.2013.003.

[40] Nathan Mulherin, Robert Haehnel. Ice engineering: Progress in evaluating surface coatings for icing control at corps hydraulic structures . . 2003.

[41] Work A, Lian Y. Progress in aerospace sciences. *Progress in aerospace sciences*. 1970;98:1-26. http://www.sciencedirect.com/science/article/pii/S0376042118300058.

[42] AeroPEL – AeroPel icephobic & omniphobic aerospace coatings. https://aeropel-technology.com/. Accessed May 18, 2020.

[43] HybridShield icephobic. https://nanosonic.com/product/hybridshield-icephobic/. Accessed May 18, 2020.

[44] Icephobic coatings, anti-ice coating and paint from ecological coatings. http://www.ecologicalcoatings.com/icephobic.html.

[45] Synavax™ hydrophobic coatings & icephobic coatings. https://www.synavax.com/hydrophobic-coatings-icephobic-coatings/. Accessed May 18, 2020.

[46] Editors Hc. Wright brothers. https://www.history.com/topics/inventions/wright-brothers. Accessed Mar 27, 2020.

[47] This day in 1906: Skepticism about the wright brothers | science 2.0. https://www.science20.com/cool-links/day_1906_skepticism_about_wright_brothers-76109. Updated 2014. Accessed Mar 27, 2020.

[48] Wright airplanes. http://www.wright-brothers.org/Information_Desk/Just_the_Facts/Airplanes/Wright_Airplanes.htm. Updated 2010.

[49] Dr. Stimson. Wright brothers stories. http://www.wrightstories.com/airplane.html. Accessed 27.3., 2020.

[50] History of aviation. . 2020. https://en.wikipedia.org/w/index.php?title=History_of_aviation&oldid=947193241. Accessed Mar 31, 2020.

[51] Benson T. Overview of the wright brothers' invention process. . 2014. https://wright.nasa.gov/overview.htm.

[52] Hawkins AJ. Airbus' new bird-plane hybrid is both fascinating and unsettling. https://www.theverge.com/2019/7/19/20700614/airbus-bird-of-prey-plane-hybrid-concept. Updated 2019. Accessed Apr 1, 2020.

[53] Airbus inspired by nature to boost aircraft environmental performance. https://www.airbus.com/newsroom/press-releases/en/2019/11/airbus-inspired-by-nature-to-boost-aircraft-environmental-performance.html. Accessed Apr 1, 2020.

[54] Biomimicry: Engineering in nature's style. https://www.airbus.com/newsroom/news/en/2018/01/biomimicry--engineering-in-nature-s-style.html. Accessed Apr 1, 2020.

[55] Airbus inspired by nature to boost aircraft environmental performance. https://www.airbus.com/newsroom/press-releases/en/2019/11/airbus-inspired-by-nature-to-boost-aircraft-environmental-performance.html. Accessed Apr 1, 2020.

[56] Rich SC. Aircraft design inspired by nature and enabled by tech. https://www.smithsonianmag.com/arts-culture/aircraft-design-inspired-by-nature-and-enabled-by-tech-25222971/. Accessed Apr 6, 2020.

[57] Birds skeleton : Twootz.com. https://twootz.com/article/Bird-Skeleton. Accessed Apr 6, 2020.

[58] Wang H, Yang Y, Guo L. Nature-inspired electrochemical energy-storage materials and devices. *Advanced Energy Materials*. 2017;7(5):1601709. https://onlinelibrary.wiley.com/doi/abs/10.1002/aenm.201601709. Accessed Apr 6, 2020. doi: 10.1002/aenm.201601709.

[59] Di Marzo Serugendo G, Anthony K, Rana O, Zambonelli F. Engineering self-organising systems. nature-inspired approaches to software engineering. . 2020. Accessed Apr 6, 2020. doi: 10.1007/b95863.

[60] Huang C, Guo Z. Fabrications and applications of slippery liquid-infused porous surfaces inspired from nature: A review. *J Bionic Eng*. 2019;16(5):769-793. doi: 10.1007/s42235-019-0096-2.

[61] *Slips.* Harvard School of Engineering and Applied Sciences: Wyss Institute; 2013.

[62] American museum of natural history | new york city. https://www.amnh.org. Accessed Mar 13, 2020.

[63] ¿Conocéis el efecto loto? . 2015. https://www.atriainnovation.com/en/what-lotus-effect-is/. Accessed Mar 13, 2020.

[64] Rui Luo. Butterfly wings .

[65] Ensikat HJ, Ditsche-Kuru P, Neinhuis C, Barthlott W. Superhydrophobicity in perfection: The outstanding properties of the lotus leaf. *Beilstein J Nanotechnol*. 2011;2:152-161. https://www.ncbi.nlm.nih.gov/pmc/articles/PMC3148040/. Accessed Feb 26, 2020. doi: 10.3762/bjnano.2.19.

[66] Sandhu A, J. Walker O, Nistal A, Leong Choy K, J. Clancy A. Perfluoroalkane wax infused gels for effective, regenerating, anti-icing surfaces. *Chemical Communications*. 2019;55(22):3215-3218. https://pubs.rsc.org/en/content/articlelanding/2019/cc/c8cc09818b. Accessed Apr 29, 2020. doi: 10.1039/C8CC09818B.

[67] The lotus effect. . 2010. https://futureprospects.wordpress.com/2010/05/17/the-lotus-effect/. Accessed Feb 26, 2020.

[68] Lotus effect. . 2019. https://en.wikipedia.org/w/index.php?title=Lotus_effect&oldid=921935640. Accessed Feb 26, 2020.

[69] Troeger A. SLIPS–Slippery liquid infused porous surfaces via fs-laser ablation. . 2018. https://www.advancedsciencenews.com/slips-slippery-liquid-infused-porous-surfaces-via-fs-laser-ablation/. Accessed Feb 26, 2020.

[70] Irajizad P, Hasnain M, Farokhnia N, Sajadi SM, Ghasemi H. Magnetic slippery extreme icephobic surfaces. *Nature communications*. 2016;7(1):13395. https://www.ncbi.nlm.nih.gov/pubmed/27824053. doi: 10.1038/ncomms13395.

[71] The history of thermal spray in a nutshell | A&A thermal spray coatings. https://www.thermalspray.com/the-history-of-thermal-spray-in-a-nutshell/. Updated 2018. Accessed Mar 13, 2020.

[72] Petrovicova E, Schadler LS. Thermal spraying of polymers. *International Materials Reviews*. 2002;47(4):169-190. https://doi.org/10.1179/095066002225006566. Accessed Feb 25, 2020. doi: 10.1179/095066002225006566.

[73] Saleem Hashmi, Gilmar Ferreira Batalha, ... Bekir Yilbas. *Comprehensive materials processing* . ScienceDirect; 2014.

[74] Thermal spray process diagram. http://bexxonglobal.com/thermal-spray-process-diagram.html. Accessed Mar 13, 2020.

[75] Assadi H, Kreye H, Gärtner F, Klassen T. Cold spraying – A materials perspective. *Acta Materialia*. 2016;116:382-407. http://www.sciencedirect.com/science/article/pii/S1359645416304530. Accessed Mar 13, 2020. doi: 10.1016/j.actamat.2016.06.034.

[76] Raletz F, Vardelle M, Ezo'o G. Critical particle velocity under cold spray conditions. *Surface and Coatings Technology*. 2006;201(5):1942-1947. http://www.sciencedirect.com/science/article/pii/S0257897206003744. Accessed May 26, 2020. doi: 10.1016/j.surfcoat.2006.04.061.

[77] Moridi A, Hassani-Gangaraj SM, Guagliano M, Dao M. Cold spray coating: Review of material systems and future perspectives. *Surface Engineering*. 2014;30(6):369-395. https://doi.org/10.1179/1743294414Y.0000000270. Accessed Mar 16, 2020. doi: 10.1179/1743294414Y.0000000270.

[78] Li W, Liao H, Wang H. 8 - cold spraying of light alloys. In: Dong H, ed. *Surface engineering of light alloys.* Woodhead Publishing; 2010:242-293. http://www.sciencedirect.com/science/article/pii/B9781845695378500087. Accessed Mar 16, 2020.

[79] Bala N, Singh H, Karthikeyan J, Prakash S. Cold spray coating process for corrosion protection: A review. *Surface Engineering*. 2014;30(6):414-421. https://doi.org/10.1179/1743294413Y.0000000148. Accessed Mar 16, 2020. doi: 10.1179/1743294413Y.0000000148.

[80] Champagne VK, Helfritch DJ. Mainstreaming cold spray – push for applications. *Surface Engineering*. 2014;30(6):396-403.

https://doi.org/10.1179/1743294414Y.0000000277. Accessed Mar 16, 2020. doi: 10.1179/1743294414Y.0000000277.

[81] Xu Y, Hutchings IM. Cold spray deposition of thermoplastic powder. *Surface & Coatings Technology*. 2006;201(6):3044-3050. http://dx.doi.org/10.1016/j.surfcoat.2006.06.016. doi: 10.1016/j.surfcoat.2006.06.016.

[82] Bush T, Khalkhali Z, Champagne V, Schmidt D, Rothstein J. Optimization of cold spray deposition of high-density polyethylene powders. *J Therm Spray Tech*. 2017;26(7):1548-1564. doi: 10.1007/s11666-017-0627-5.

[83] Ravi K, Ichikawa Y, Deplancke T, Ogawa K, Lame O, Cavaille J. Development of ultra-high molecular weight polyethylene (UHMWPE) coating by cold spray technique. *J Therm Spray Tech*. 2015;24(6):1015-1025. https://hal.archives-ouvertes.fr/hal-01804751. doi: 10.1007/s11666-015-0276-5.

[84] Ravi K, Sulen WL, Bernard C, Ichikawa Y, Ogawa K. Fabrication of micro-/nano-structured super-hydrophobic fluorinated polymer coatings by cold-spray. *Surface & Coatings Technology*. 2019;373:17-24. http://dx.doi.org/10.1016/j.surfcoat.2019.05.078. doi: 10.1016/j.surfcoat.2019.05.078.

[85] Gordon England. Cold spray coating process. https://www.gordoneng-land.co.uk/coldspray.htm. Updated 2018. Accessed May, 2020.

[86] Kúdela J, Ihracký P. Influence of diverse conditions during accelerated ageing of beech wood on its surface roughness. . 2014. Accessed May 4, 2020.

[87] Semprebon C, McHale G, Kusumaatmaja H. Apparent contact angle and contact angle hysteresis on liquid infused surfaces. *Soft Matter*. 2017;13(1):101-110. https://pubs.rsc.org/en/content/articlelanding/2017/sm/c6sm00920d. Accessed May 12, 2020. doi: 10.1039/C6SM00920D.

[88] Martin i Vilardell A. *Functionalized coatings by cold spray for joint prosthesis.* University of Barcelona; 2016.

APPENDIX A: PROCESS DEVELOPMENT

Pre-trials conducted using thermoplastic polyolefin-based alloy (PLASCOAT PPA 571 HES) and Low-density polyethylene powder (Plascoat LDPE) using the LPCS and HPCS guns did not produce any coating due to low powder melting temperature. With the LPCS, the original nozzle design was used. After pre-trials, the original nozzle design for the The DYMET model 403K was modified to a rectangular-shaped nozzle to enhance dispersion during this study. The modified gun nozzle is shown is Figure 48. The first trials with successful dispersion/adhesion were conducted with Polypropylen, Coathylene PB 0580, which has a higher melting temperature, using both HPCS and LPCS (modified nozzle).

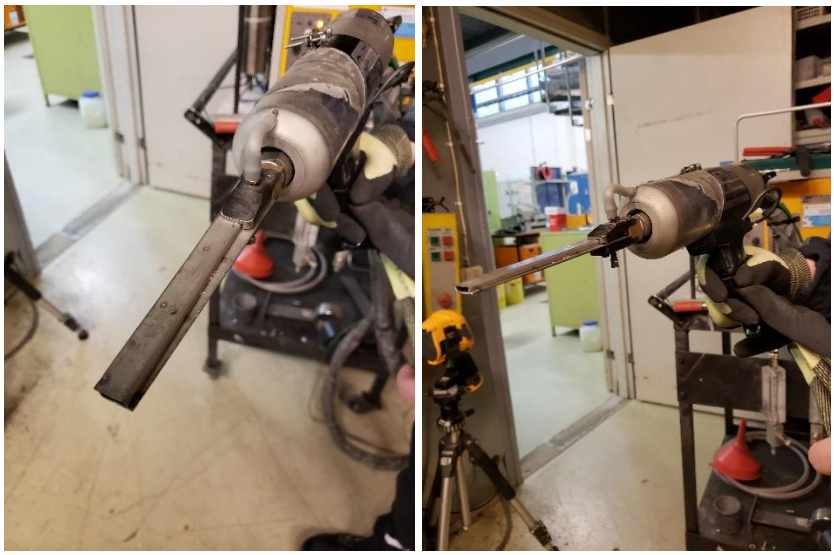

Figure 48. *LPCS gun nozzle showing modified nozzle with rectangular shape*

The following points are noted from the process:

1. Data obtained using the HPCS gun are successful. Structures achieved are porous, infusible, and showed hydrophobic properties. Coatings produced with the HPCS gun are durable, have good adhesion and oil-lockability.
2. Based on HPCS data, porosity increases with spraying distance and increases with smaller spraying angle (i.e. tilting spraying gun).
3. Technical difficulties were encountered with the LPCS gun, include persistent nozzle clogging and inconsistent dispersion patterns. Some coatings were produced. However, coating produced with low pressure has poor adhesion and did not withstand sample preparation for further analysis.

4. The LPCS gun has too high operating temperature for the selected polymer powders but gas heating can be turned off (resulting in poor adhesion).
5. Using a heating element to keep the substrate at a constant temperature causes undesirable polymer degradation. This is due to the high minimum temperature initially needed for adhesion. Additionally, this technique is not recommended for industry use (e.g. for spraying large fields).

Tables 8 through 11 are produced with low pressure cold spray. Table 8 shows the spraying parameters for the first set. Sample 1 coating has surface asperities that can be observed with the naked eye while Sample 2 coating appears smoother and more consistent. No coating is produced for Samples 3, 4 and 5. It is thought that the low gas temperature did not allowing for powder softening and adhesion to the steel substrate. Figures 49 and 50 show Sample 1 and Sample 2, respectively.

***Table 8**: Low pressure Set 1*

Sample (Trial)	Gas Temp. (ºC)	Gas Pressure (bar)	Powder Feeding	Plate Temp. (ºC)	Spray Speed
1	224	4.2	3.5	120	slow
2	224	4.2	3.5	120	fast
3	21	4.2	3.5	120	slow
4	21	5.2	3.5	120	slow
5	21	5.2	4	120	slow
Powder (Polypropylen, Coathylene PB 0580, d_{50} < 50 microns, white), Plate (Steel, Grit-blasted aluminum oxide F24), Spray gun (DYMET model 403K). Substrates were sprayed with an operator. Plate is left to cool during spraying (i.e. pre-heated).					

Figure 49. *Sample 1*

Figure 50. *Sample 2*

Additionally, Sample 1 and 2 do not appear porous. It is thought that the high operating temperature of the LPCS gun caused powdering melting and smoothening of the coating. The minimum operating condition for the LPCS are approximately 4.2 bar and 224 to 226 °C. Operating below 4.2 bar will atomically turn off heating for the LPCS gun, resulting in lack of powder softening and, therefore, poor adhesion.

Table 9 shows spraying parameters for the second set with LPCS. Sample 6 and 8 produced coatings on parts of the substrate (the nozzle was clogged during spraying due to powder melting). Sample 7 produced coating that was removed during spraying due to poor adhesion. It is thought that Sample 9 did not produce coating due to melting of the powder inside the nozzle. The coatings are shown in Figure 51 and Figure 52.

Table 9*: Low pressure Set 2*

Sample (Trial)	Gas Temp. (°C)	Gas Pressure (bar)	Powder Feeding	Plate Temp. (°C)	Spray Speed
6	224	4,2	3,5	100	slow
7	224	4,2	3,5	80	slow
8	224	4,2	3,5	90	slow
9	224	4,2	3,5	95	slow
Powder (Polypropylen, Coathylene PB 0580, d_{50} < 50 microns, white), Plate (Steel, Grit-blasted aluminum oxide F24), Spray gun (DYMET model 403K). Substrates were sprayed with an operator. Plate is left to cool during spraying (i.e. pre-heated). Number of Passes = 1					

The results from this spraying session shows that adhesion of Polypropylen coating at the specified parameters occurs when the plate temperature is above 90 °C. As shown in the figures below, Sample 8 has poor apparent adhesion while Sample 6 coating adhered to the substrate as it should. It should be noted that “apparent adhesion” does not indicate good or bad coating durability in erosive condition but is rather a term used to describe if powder adhered immediately after spraying.

Figure 51. *Sample 6*

Figure 52. *Sample 8*

Table 10 shows the parameters for the third set. Increasing gas pressure to 5,2 bars in trial 10 resulted in thinner coating compared to trials 11 and 12. Increasing powder feeding to 4 also resulted in thin coating compared to Sample 11. Only parts of the substrates

are sprayed due to technical issues with the LPCS gun. Plate is left to cool during spraying (i.e. pre-heated). Figures 53 and 54 show the coatings.

***Table 10**: Low pressure Set 3*

Sample (Trial)	Gas Temp. (ºC)	Gas Pressure (bar)	Powder Feeding	Plate Temp. (ºC)	Spray Speed
10	226	5,2	3,5	120	slow
11	225	4,4	3,5	120	slow
12	225	4,4	4	120	slow
Powder (Polypropylen, Coathylene PB 0580, d_{50} < 50 microns, white), Plate (Steel, Grit-blasted aluminum oxide F24), Spray gun (DYMET model 403K). Substrates were sprayed with an operator. Plate is left to cool during spraying (i.e. pre-heated). Number of Passes = 1					

Figure 53. *Sample 10*

Figure 54. *Sample 11 (bottom), Sample 12 (top)*

The next spraying session shown in Table 11 is conducted to the same substrate. First, the coating 14 is produced to the middle of the substrate using Trial 14 parameters. Then, the right end of the substrate is heated to Plate Temperature and spraying is done with parameters for Trial 15. Finally, the left end of the substrate is heated, and spraying is done with Trial 13 parameters. Figure 55 shows the effect of powder feeding, and re-heating the substrate resulting in smoothening of the coating.

***Table 11**: Low pressure Set 4*

Sample (Trial)	Gas Temp. (ºC)	Gas Pressure (bar)	Powder Feeding	Plate Temp. (ºC)	Spray Speed
13	225	4,2	3	120	fast
14	225	4,4	3,5	120	fast
15	225	4,2	3,5	120	fast
Powder (Polypropylen, Coathylene PB 0580, d_{50} < 50 microns, white), Plate (Steel, Grit-blasted aluminum oxide F24), Spray gun (DYMET model 403K). Substrates were sprayed with an operator. Plate is left to cool during spraying (i.e. pre-heated). Number of Passes = 3					

***Figure 55.** Samples 13 (left end), 14 (middle) and 15 (right end)*

Table 12 shows the parameters for the fourth set. Substrates were sprayed using a robot. The spray gun moves at 2 mm step increments (half nozzle width). A heating element is used to keep the temperature at a constant value. Trial 19 produced a thin coating with few surface asperities. Coating on Sample 18 lacks consistency. Trial 17 produced a very thin coating. Trial 16 did not produce any coating. Figure 56 and Figure 57 show Sample 17 and 18, respectively.

***Table 12**: Low pressure Set 5*

Sample (Trial)	Gas Temp. (ºC)	Gas Pressure (bar)	Powder Feeding	Plate Temp. (ºC)	Speed (mm/s)
16	228	4,2	3,5	120	166
17	228	4,2	3,5	120	100
18	228	4,2	3,5	120	50

Powder (Polypropylen, Coathylene PB 0580, d_{50} < 50 microns, white), Plate (Steel, Grit-blasted aluminum oxide F24), Spray gun (DYMET model 403K). Substrates were sprayed using a robot (2 mm steps). Spraying distance = 15 mm. Heating element is used. Number of Passes = 1

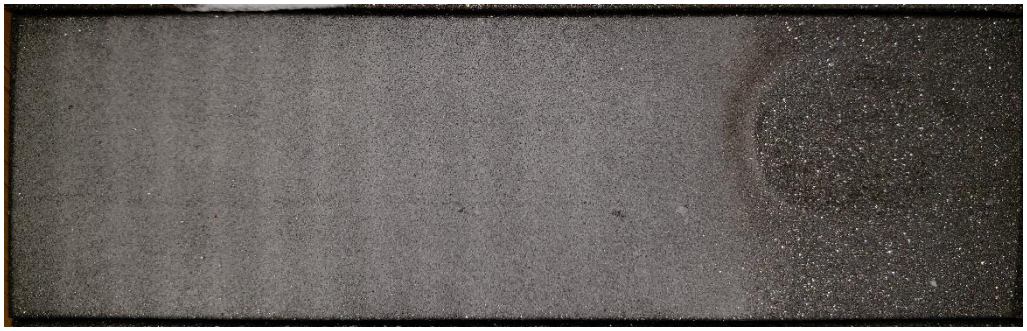

Figure 56. *Sample 17*

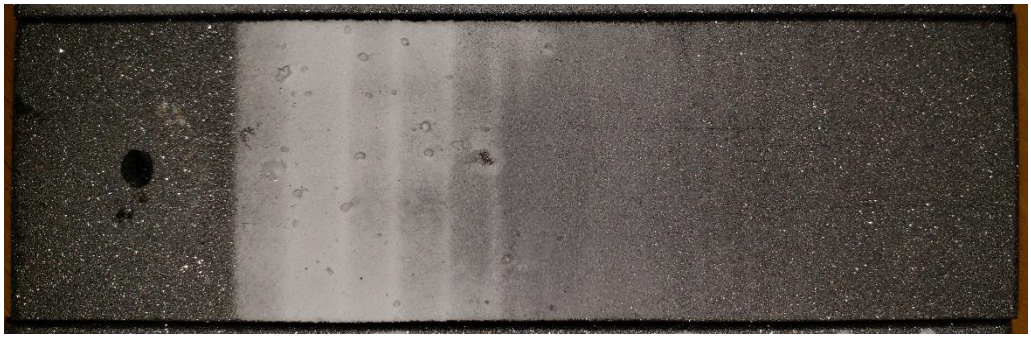

Figure 57. *Sample 18*

The next sets of results (Table 13 and 14) are produced with high pressure. Table 13 shows data for the first spraying session using HPCS gun using a robot. Spray gun moves at 5 mm step increments. Note the unit for speed is m/min. In both trials, the polymer coating was being degraded due to the heating element (i.e. continuous plate heating). Figure 58 and Figure 59 show samples 19 and 20, respectively.

Table 13*: High pressure Set 1*

Sample (Trial)	Gas Temp. (ºC)	Gas Pressure (bar)	Powder Feeding	Plate Temp. (ºC)	Speed (m/min)
19	150	15	4 rpm	115	10
20	150	15	4 rpm	135	10
Powder (Polypropylen, Coathylene PB 0580, d_{50} < 50 microns, white), Plate (Steel, Grit-blasted aluminum oxide F24), Spray gun (Plasma PCS-100). Substrates were sprayed using a robot (5 mm steps). Spraying distance = 40 mm. Heating element is used. Number of Passes = 3					

Figure 58. *Sample 19*

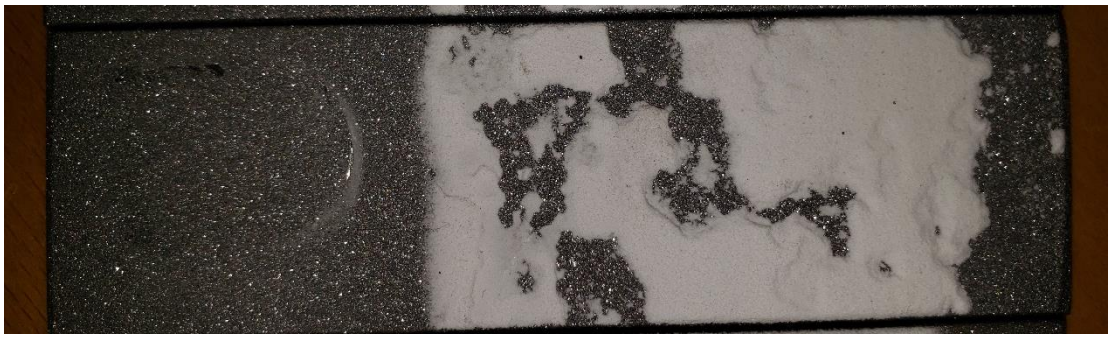

Figure 59. *Sample 20*

During the next trials, the heating element is removed. Spraying is done with different gun distances and angle. During Trial 24, the gun is slightly tilted approximately 30 degrees downwards. Figure 60 shows Samples 21 through 24. Specimen of the samples were taken for further analysis and tests (microscope, stability tests, contact angle).

Table 14*: High pressure Set 2*

Sample (Trial)	Gas Temp. (°C)	Gas Pressure (bar)	Powder Feeding	Plate Temp. (°C)	Speed (m/min)	Dist. (mm)
21	150	15	4 rpm	135	10	40
22	150	15	4 rpm	135	10	50
23	150	15	4 rpm	135	10	60
24	150	15	4 rpm	135	10	60; tilted
Powder (Polypropylen, Coathylene PB 0580, d_{50} < 50 microns, white), Plate (Steel, Grit-blasted aluminum oxide F24), Spray gun (Plasma PCS-100). Substrates were sprayed using a robot (2 mm steps). Number of Passes = 3						

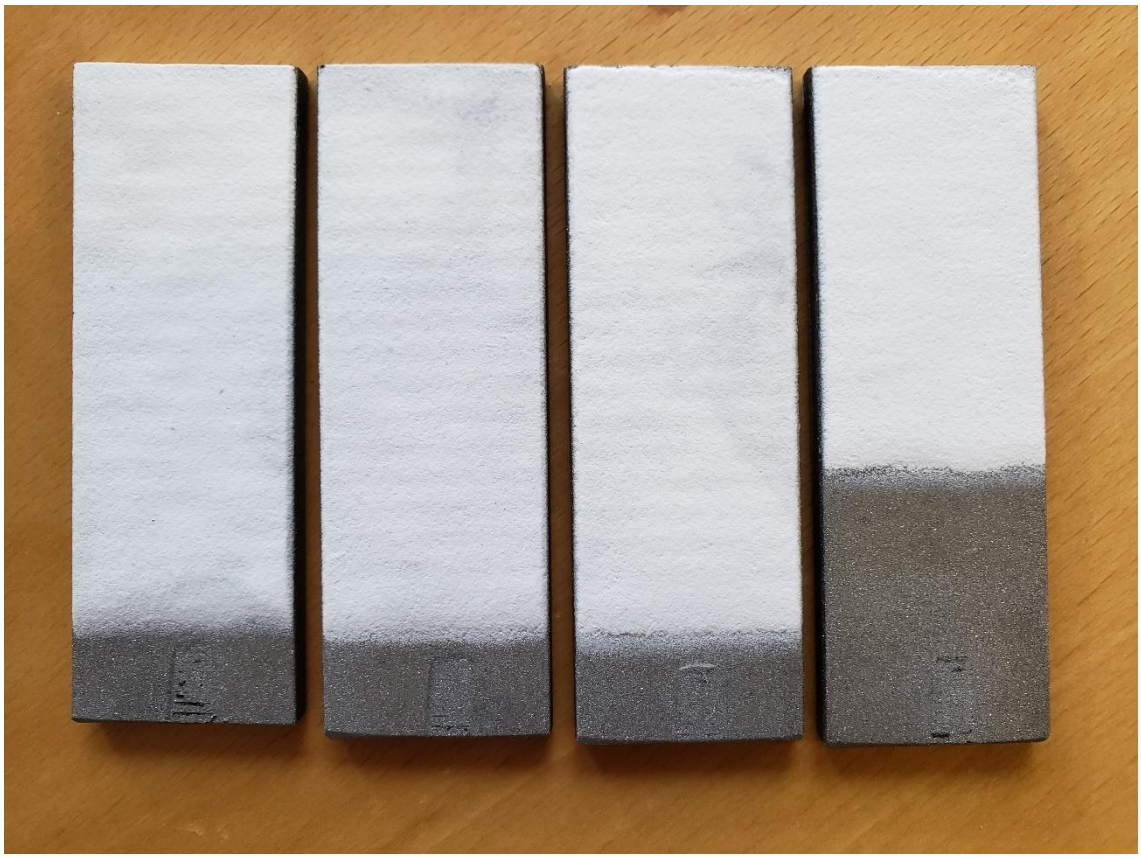

Figure 60. *Samples 21 (leftmost), Sample 22 (middle left), Sample 23 (middle right) and Sample 24 (rightmost)*